Non−linear Aanalysis of Energy Transfer in Tb^{3+} Doped Glasses

（Tb3+ 添加ガラスにおける励起エネルギー伝達の非線形解析）

１９９４年３月

埼玉大学大学院理工学研究科

物質科学専攻（指導教授　山田興治）

外岡和彦

Non-Linear Analyses of Energy Transfer in Tb^{3+}-Doped Glasses

by Kazuhiko Tonooka

Abstract

Transfer of electronic excitation between rare-earth ions were theoretically and experimentally studied. The basic theory for this process was developed initially by Förster for multi-polar interaction. Models for the fluorescence under the influence of energy transfer from energy donors to energy acceptors were presented to remove the difficulties with the Förster model. Consideration of the non-linear effect associated with the excitation of acceptors resulted in the non-linear model. The non-exponential fluorescence decays following pulsed excitation and the steady-state fluorescence of Tb^{3+}-doped glasses were examined by means of the non-linear model, giving a good agreement between experimental results and expectations from the model. In spite of the good agreement, the averaging of the population of active ions and the approximation of interaction to a simplified one-to-many interaction used in the non-linear model, were suggested to be inadequate to evaluate the status of the system. Consequently, the non-linear model was developed into a stochastic model by discriminating all active ions and by introducing the quantization of energy involved in all transitions. The connection of the elementary process of pair-transfer to the macroscopic behavior of the donor-acceptor system was explicitly formalized without any approximation for the first time. It was shown that the stochastic model gave a better fit between theoretical expectations and experimental results of the Tb-Nd glass system. Values of the parameters obtained from the analysis were examined to check the validity of the models. The stochastic model was found most acceptable to explain the system consisting of donors and acceptors with complex interaction.

Non-Linear Analyses of Energy Transfer in Tb^{3+}-Doped Glasses

by Kazuhiko Tonooka

contents

1. Introduction

Energy transfer of electronic excitation from one ion to another has been attracting attention both for theoretical interest and for practical use such as phosphors and lasers. The efficiency of luminescence will be improved (1) by choosing the host matrix which gives stronger emission, (2) by increasing the activator concentration, and (3) by utilizing the energy transfer. Higher activator concentration is possible for glasses for they are good solvents of metallic ions, although, it brings about self-concentration quenching. Self-concentration quenching is the phenomenon whereby luminescence intensity decrease with increasing activator concentration. The self-concentration quenching of the luminescence from the $^5D_3$ state of Tb^{3+} ions is mainly due to the energy transfer between Tb^{3+} ions. A overview of several energy transfer processes are shown in Fig.1. Energy transfer means that an excited ion, usually called a donor, transfers its excitation energy to another ion, called the acceptor. The absorption and emission of photon radiation by the rare-earth ions has been considered a one-ion process, however, the energy transfer is a many-ion process, mainly a two-ion process, as explained briefly in the figure.

(a) In this resonant energy transfer process, ion A (the donor) goes from its excited state A^* to its ground state A and thereby excites another ion, the acceptor, from its ground state B to its excited state B^*. In this process energy is fully conserved, meaning that the $A^* \rightarrow A$ transition and $B \rightarrow B^*$ transition have the same energy.

(b) Energy migration is a process in which the excitation of a donor moves around between donors in a random-walk manner.

(c) In phonon-assisted energy transfer, there is a considerable mismatch in energy between the acceptor and the donor. Under the conditions shown in the left figure, ion B is excited to B^* and a phonon $\hbar\omega$ is emitted to conserve energy. If the energy of the $B \rightarrow B^*$ transition is larger than the transition energy of $A^* \rightarrow A$, the missing energy has to be supplied by a phonon, as shown in the right figure.

(d) Stepwise up-conversion is a process in which two successive transitions in the donor system excite one acceptor ion to an higher energy state, approximately twice the energy. A first photon is used to excite the ion from the B state to B^* state (resonantly or phonon assisted) and a second photon is used to reach the C^* state. It is important that we can produce visible radiation from infrared radiation utilizing this mechanism.

The basic theory of energy transfer was given by Förster [1][2] and Dexter [3] Various models for the energy transfer taking account of multi-polar interactions [3][4], exchange interaction [3][4], diffusion of energy [5][6] and migration of energy [6][7] have been developed. The fluorescence decay curves under the influence of energy transfer have been analyzed by Förster-like models, in which the averaged population of donors was treated by a linear rate equation. Förster obtained a solution by integrating the energy transfer rate of a donor-acceptor pair for a large volume, disregarding the excitation of acceptors. However, the population of excited acceptors is expected to play an important role to the energy transfer process with increase of acceptors. There are several possible models such as Inokuti-Hirayama model [4], cascade models [8,9], discrete shell model [10] and sum of exponential model [11] for the non-exponential decay curves of donor fluorescence in particular conditions. The Inokuti-Hirayama model, which is given as an extension of the Förster model for multi-polar interaction, is most widely used for the analysis of donor fluorescence after a pulsed excitation. Although, none of them give general solution for all cases. A good bibliography on this field was prepared by Los Alamos National Laboratory [12].

Those old theories have two distinct problems: One is the infinite energy transfer rate which appears at the starting point of the decay curve, and the other is that they cannot be applied to phenomena which takes place after the time scale longer than the relaxation time of the system. Comparatively little attention has been given to the fluorescence in a steady-state. These problems are mainly brought by the linear approximation of the rate equation for the donor population and by the distribution function which assumes a completely random spatial distribution of interacting ions even within the ionic radius of the concerning active ion It is preferable to assume that there exist no acceptors within the range of the nearest neighbor distance of the donor and that the transfer rate of the donor is finite as a macroscopic value The modification of acceptor distribution was already suggested as an approach to form a realistic distribution of active ions by H.Dornauf et al.[13] and S.R.Rotman et al.[14]

There were many reports on the energy transfer between rare-earth ions such as $Tb^{3+} \rightarrow Dy^{3+}$ [15,16], $Tb^{3+} \rightarrow Eu^{3+}$ [15,16,17], $Tb^{3+} \rightarrow Sm^{3+}$ [15,16], $Tb^{3+} \rightarrow Tm^{3+}$ [15,16,18], $Tb^{3+} \rightarrow Pr^{3+}$ [15,16], $Tb^{3+} \rightarrow Er^{3+}$ [15,16,19] and $Tb^{3+} \rightarrow Ho^{3+}$ [15,16] Typical optical transitions of rare-earth ions are due to transitions in the inner shielded 4f

shell For this reason the fluorescence of rare-earth ions is influenced much smaller by the surrounding crystalline field than is the fluorescence of other activators having transitions in outer electron shells. Therefore, the fluorescence of rare-earth ions in glass is expected to be quite similar to that in crystals. Thus one can estimate the energy levels of rare-earth ions in glasses from the Dieke diagram shown in Fig 2. The main difference between the fluorescence of rare-earth ions in glasses and that in crystals is the inhomogeneous broadening in spectra.

In this study, more comprehensive models were presented in order to remove the difficulties with old models for the donor fluorescence under the influence of energy transfer These models are based on a coupled non-linear rate equation taking the excitations both of donors and of acceptors into consideration [20]. Steady state and transient response of the fluorescence intensity from the $^5D_3$ state of Tb^{3+} ions in glasses were analyzed using the non-linear model. Numerical calculations showed that the non-linear model gave non-exponential decay curves similar to the famous Inokuti-Hirayama equation. A good agreement was obtained between theory and experimental results. It is a significant advantage of the non-linear model that it gives a consistent interpretation of the response of donor fluorescence both in steady and in transient states from the elementary process of pair-transfer. In spite of the agreements obtained, the non-linear model looked still inadequate to explain the donor-acceptor system from a theoretical point of view. This inadequacy of the model seemed to be resulted from the approximation of the complex interaction to a simplified one-to-many interaction. Then the non-linear model was developed into a stochastic model in which the transfers of energy from donors to acceptors were stochastically calculated without approximations. A computer simulation based on the stochastic model was carried out to analyze the donor fluorescence of the Tb-Nd glass system

The second chapter deals with the basic theory of energy transfer for a donor-acceptor pair and extensions to a macroscopic system consisting of many donors and acceptors with multi-polar interaction. The physical picture and the mathematical treatments of the Förster model is interpreted as an approximation of the complex interaction to the simplified one-to-many interaction. Importance of the non-linearlity associated with the excitations of active ions and the introduction of the non-linear term into the rate equation are described in comparison with the Förster model. The non-linear model for the donor fluorescence is presented to remove the difficulties with the Förster model.

In the third chapter, experimental results on the donor fluorescence are analyzed using the non-linear model. It is shown that the donor fluorescence in steady state and transient response from Tb^{3+} ions in glasses are consistently understood by the non-linear model, whereas the Forster-like models can be applied only to the transient response. Decay characteristics by the non-linear model are examined comparing with those by the Förster model, giving a considerable difference in the short time behaviors of their fluorescence decays between these models.

The fourth chapter describes computer simulations applied to the analysis of energy transfer. A stochastic model for the donor fluorescence is proposed as an extension of the non-linear model to consider the complex interactions between donors and acceptors without approximations. The discrimination of individual active ions and the quantization of energy associated with all transitions are identical to the stochastic model. Monte Carlo simulations on a computer are used for the evaluation of fluorescence decays based on the stochastic model. Better agreements are reported between the simulated results by a computer and the experimental results on Tb^{3+}-doped glasses.

The fifth chapter focuses on the origins for the non-exponential responses and the effect of energy back-transfer. Theoretical investigations of the non-linear model, the stochastic model the Förster model concludes that the non-exponential responses of the donor fluorescence, which is the main character of the system occurring energy transfer, is better understood as a result of the non-linearity in the dynamics of energy transfer. Considerable presence of energy back transfer is suggested from the spectral investigation of Tb^{3+} ions in glasses and from the evaluation of the energy relaxation of acceptors with and without considering the back transfer.

Concluding remarks are described in the sixth chapter. The stochastic model is found most acceptable to account for the macroscopic behavior of donor fluorescence based on the fundamental process of energy transfer between a donor and an acceptor. It is also concluded that the discrimination of individual active ions and the quantization of transferred energy are essential to formalize the system consisting of donors and acceptors with complex interaction. Usefulness and limitations of a computer simulation are mentioned to carry out the analysis of energy transfer based on the stochastic model.

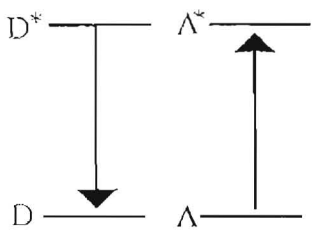

(a) Resonant Energy Transfer

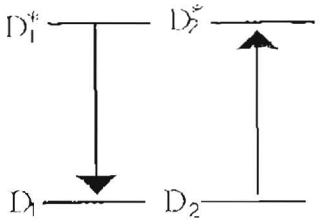

(b) Energy Migration

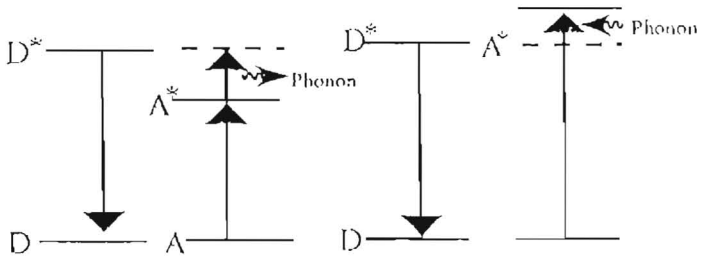

(c) Phonon Asisted Energy Transfer

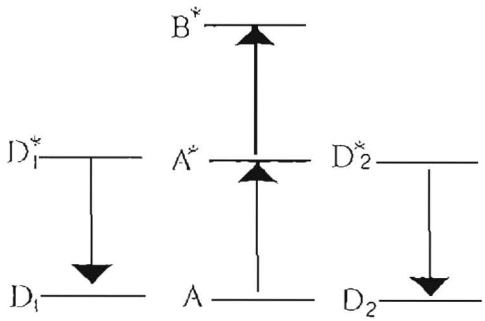

(d) Stepwise energy up-conversion.

Fig.1. Diagrams of several energy transfer processes. (a) Resonant energy transfer. (b) Energy migration, by which the excitation moves between donors. (c) Phonon assisted energy transfer with the emmission or absorption of a phonon. (d) Stepwise energy up-conversion.

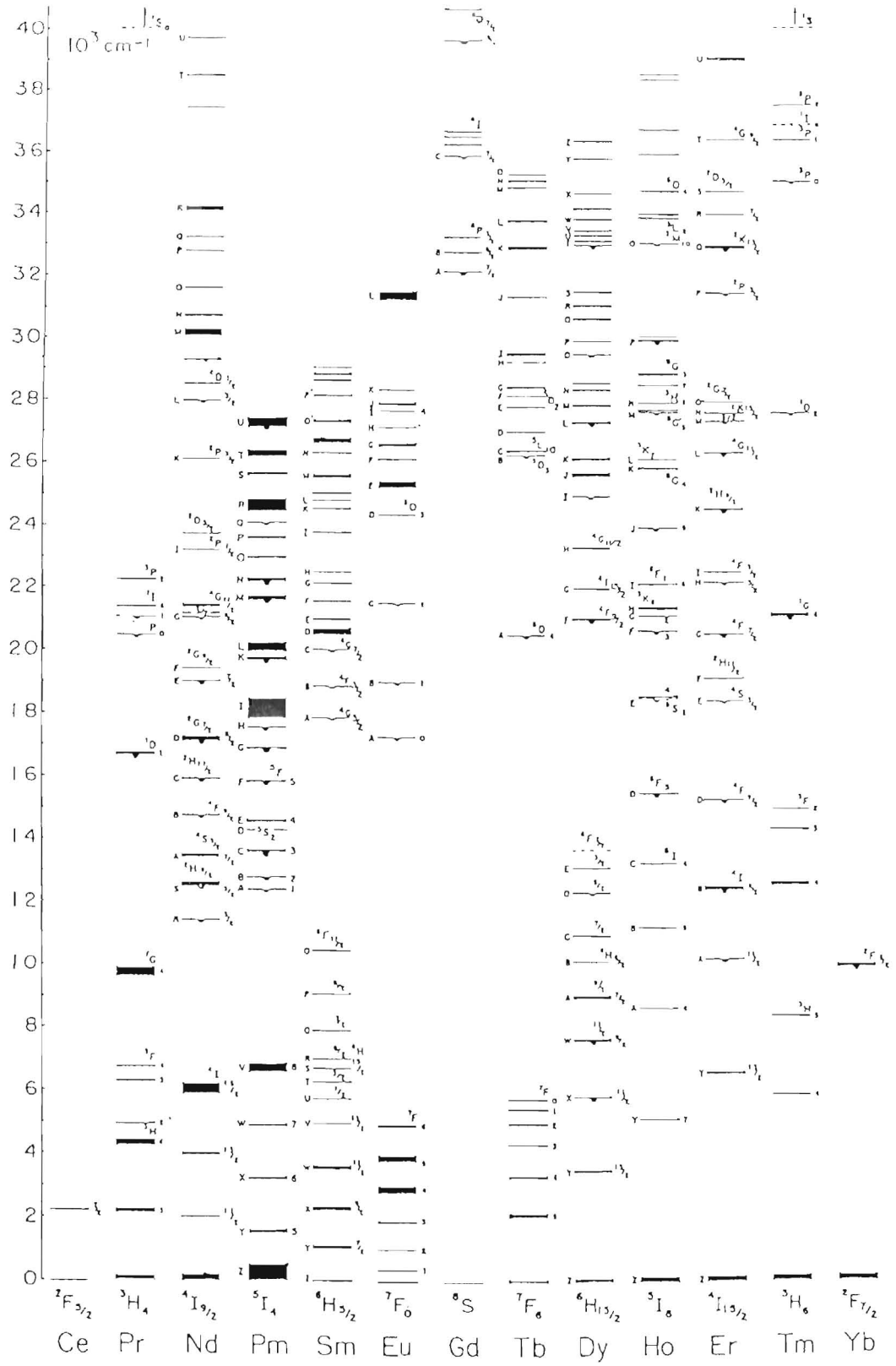

Fig.2. Dieke diagram: energy levels of trivalent rare-earth ions in $LaCl_3$ lattice
Levels labeled with black half-circles are levels from which luminescence is observed.

2. Theories

2.1. Basic theory of energy transfer

Dexter derived the following expression for the probability of resonant energy transfer for a donor-acceptor pair via an electric dipole-dipole interaction as,

$$P = \frac{3\hbar^4 c^4 \, Q_a k_R}{4\pi n^4 r^6} \left(\frac{\varepsilon}{\kappa^{1/2} \varepsilon_c} \right)^4 \int \frac{f_d(E) \, F_a(E)}{E^4} dE \quad , \qquad (1)$$

where n is the refractive index, r is the distance between the donor and the acceptor, c is the velocity of light, κ is the dielectric constant, ε_c is the permittivity of the medium, k_R is the radiative transition probability for the donor, Q_a ($= \int \sigma_a(E) dE$) is the energy integral of the optical cross-section $\sigma_a(E)$ in the absorption band, $f_d(E)$ is the normalized emission spectrum of the donor and $F_a(E)$ is the normalized absorption spectrum of the acceptor. We can set the quantity $(\varepsilon / \kappa^{1/2} \varepsilon_c)$ equal to unity in the numerical evaluation. Since a donor transfers energy to its nearby acceptors and an acceptor obtains energy from its nearby donors, the expression for the energy transfer should reflect the local distribution of the distances between such interacting ions. Extending eq.(1) for the multi-polar interaction, one can rewrite it as

$$P(r) = k_R \left(\frac{R_0}{r} \right)^s \quad , \qquad (2)$$

where

$$R_0^s = \frac{3\hbar^4 c^4}{4\pi n^4} \left(\frac{\varepsilon}{\kappa^{1/2} \varepsilon_c} \right)^4 \int \sigma_a(E) dE \int \frac{f_d(E) \, F_a(E)}{E^4} dE \quad , \qquad (3)$$

and s is 6,8,10 for dipole-dipole (d-d), dipole-quadrupole (d-q) and quadrupole-quadrupole (q-q) interactions, respectively. The parameter R_0 is usually called the critical distance of energy transfer.

Consider a system in which donors and acceptors are randomly distributed as shown in Fig.3 (a). The distribution of rare-earth ions doped in glassy medium is a typical case. Since donors and acceptors are usually cations, there exist such anions as O^{2-} among active ions. In the figure, however, these anions were omitted for clarity. The probability of energy transfer from donors to acceptors depends on the distance between them. Since a donor transfers energy to its nearby acceptors and an acceptor obtains energy from its nearby donors, the expression of the

energy transfer should reflect the local distribution of the distances between such interacting ions. Figure 3 (b) shows the schematic paths of the energy transfer from one specific donor to nearby acceptors for the same distribution of Fig 3 (a). Suppose that there are N_a acceptors which can receive energy from the donor. The probability of energy transfer for the donor is given by

$$P_d = k_R R_0^s \sum_{k=1}^{N_a} R_{ak}^{-s} \quad , \quad \cdots\cdots (4)$$

where R_{ak} is the distance between the donor and the k-th acceptor. Similarly, the probability for one specific acceptor obtaining energy from nearby donors, as shown in Fig.3 (c), is given by

$$P_a = k_R R_0^s \sum_{k=1}^{N_d} R_{dk}^{-s} \quad , \quad \cdots\cdots (5)$$

where N_d is the number of donors which can give energy to the acceptor and R_{dk} is the distance between the acceptor and the k-th donor. The migration, the diffusion and the back-transfer of the excitation [21,22] were neglected here. One can see from eqs (4) and (5) that the probabilities of energy transfer for each donor and acceptor are usually different, therefore these energy transfer rates should be distinguished in forming rate equations.

2.2. Förster model

At first, the Förster model should be reviewed, since it helps us to understand the fundamentals and the phenomenology of the donor fluorescence in a macroscopic system. Approximating the complex interactions between many donors and acceptors to the simplified interaction between a donor and acceptors, Förster analyzed the donor fluorescence with with the following rate equation for the population of donors,

$$\frac{d\rho_d(t)}{dt} = -k_R \rho(t) - k_R \sum_{k=1}^{N_a} \left(\frac{R_0}{R_k}\right)^6 \rho_d(t) \quad , \quad \cdots\cdots (6)$$

where $\rho_d(t)$ is the population of the donor, k_R is the radiative transition rate of donors, N_a is the number of acceptors, R_k is the distance between the donor and the k-th acceptor, R_0 is the

critical distance of energy transfer. This rate equation is restricted to the dipole-dipole interaction The excitation of acceptors were disregarded in the Förster model.

We begin with the following rate equation extended to the multi-polar interaction ,

$$\frac{d\rho_d(t)}{dt} = -k_R \rho_d(t) - k_R \sum_{k=1}^{N_a} \left(\frac{R_0}{R_k}\right)^s \rho_d(t) \quad , \quad \cdots\cdots (7)$$

where S is 6, 8 and 10 for the dipole-dipole, the dipole-quadrupole and the quadrupole-quadrupole interactions. The excitation of acceptors were disregarded in the Förster model The exact solution of eq (7) can be written in the form

$$\rho_d(t) = \rho_d(0) \exp\left(-k_R t - k_R R_0^s \sum_{k=1}^{N_a} R_k^{-s} t\right) \quad , \quad \cdots\cdots (8)$$

or

$$\rho_d(t) = \rho_d(0) \exp(-k_R t) \prod_{k=1}^{N_a} \exp(-k_R R_0^s R_k^{-s} t) \quad , \quad \cdots\cdots (9)$$

Introducing the distribution function w(r) , Förster obtained the macroscopically averaged value of $\rho_d(t)$ as

$$\overline{\rho(t)} = \rho_0 \exp(-k_R t) \lim_{R_g \to \infty} \left[\int_0^{R_g} w(R) \exp\left(-k_R \left(\frac{R_0}{r}\right)^s t\right) dr\right]^N \quad , \quad \cdots\cdots (10)$$

where

$$N = \frac{4}{3} \pi R_g^3 C_a \quad , \quad \cdots\cdots (11)$$

C_a is the acceptor concentration and the distribution function of acceptors around the donor is normalized such that

$$\int_0^{R_g} w(r)\, dr = 1 \quad \cdots\cdots (12)$$

It is convenient to rewrite eq. (10) as

$$\overline{\rho(t)} = \rho(0) \exp(-k_R t) \lim_{R_g \to \infty} [J(t)]^N \quad , \quad \cdots\cdots (13)$$

where

$$J(t) = \int_0^{R_g} w(r) \exp(-k_R t R_0^s r^{-s})\, dr \quad \cdots\cdots (14)$$

Then he assumed that the distribution of acceptors around the concerning donor was completely proportional to r^2 for all r, as shown in Fig.4. Putting the distribution function as

$$w(r) = \frac{4\pi r^2}{V} \quad , \qquad (15)$$

where

$$V = \frac{4}{3}\pi R_g^3 \quad , \qquad (16)$$

one can write function J(t) as

$$J(t) = \frac{4\pi}{V}\int_0^{R_g} r^2 \exp(-k_R t R_0^s r^{-s})\, dr \qquad (17)$$

Expanding the eq.(17) in a power series of t and neglecting the higher order term than $t^{3/s}$, he obtained

$$J(t) \approx 1 - \frac{4}{3}\pi C_B R_0^3 \Gamma(1-3/s)\frac{1}{N}(k_r t)^{3/s} \qquad (18)$$

The procedure reducing to equation (18) is explained in the appendix. We should be aware that this approximation leading to equation (18) will limit the validity of the Förster model. Making use of eq.(11), eq. (13) and the formula

$$\exp(x) = \lim_{N\to\infty}\left(1+\frac{x}{N}t\right)^N \quad , \qquad (19)$$

one get the approximated relation

$$\overline{\rho(t)} = \rho(0)\exp(-k_R t)\exp\{-\frac{4\pi}{3}C_B\Gamma(1-3/s)R_0^s(k_R t)^{3/s}\} \qquad (20)$$

This is the decay function initially obtained by Förster for the donor fluorescence. Putting

$$C_0 = \frac{3}{4\pi}R_0^{-3} \quad , \qquad (21)$$

we can get the Inokuti-Hirayama equation,

$$\phi(t) = \phi(0)\exp[-k_R t - \Gamma(1-\frac{3}{s})\frac{C_B}{C_0}(k_R t)^{3/S}] \qquad (22)$$

Sophisticated treatments and approximations outlined above are inevitable to obtain the results in the Förster model, since the summed transfer rate in eq. (7),

$$k_R R_0^s \sum_{k=1}^{N_B} R_k^{-s} \quad , \qquad (23)$$

becomes infinite when it is calculated with the distribution function $W(r)$ proportional to the donor-acceptor distance r for all r. Mathematical approximations used in the Förster model may reduce the theoretical consistency of it. Thus, we should notice that the Inokuti-Hirayama equation is not a theoretical equation but an approximated one.

2.3. Non-linear model

Unlike the Förster model, the time dependent population of acceptors in excited state and the excitation term for analyzing the steady state fluorescence were taken into consideration in this model. The rate equation for the populations of donors and acceptors, $\rho_d(t)$ and $\rho_a(t)$ are given by [20]

$$\begin{cases} \dfrac{d\rho_d(t)}{dt} = g(1-\rho_d(t)) - (k_R+k_N)\,\rho_d(t) - k_{Td}\,(1-\rho_a(t))\,\rho_d(t) \\ \dfrac{d\rho_a(t)}{dt} = k_{Ta}\rho_d(t)\,(1-\rho_a(t)) - k_A\,\rho_a(t) \end{cases} \qquad \cdots\cdots (24)$$

where k_N is the energy relaxation rate of the donors by non-radiative transitions, k_A is the energy relaxation rate of the acceptors, k_{Td} is the energy transfer rate from a donor to acceptors, k_{Ta} is the energy transfer rate from donors to an acceptor and g is the excitation rate of the donors. Addition of the excitation term for donors is necessary to analyze the fluorescence in a steady state. The quantities k_{Td} and k_{Ta} are the macroscopic values corresponding to eqs.(4) and (5) respectively and assumed to be finite. Formalization of the rate equation as ordinary differential equations is permitted by the introduction of finite k_{Td} and k_{Ta}. The macroscopic model described by equation (24) is shown schematically in Fig.5 It is possible to obtain a linear equation equivalent to the rate equation of the Forster by approximating the equation (24) to a linear form. The non-linear product $\rho_d(t)\cdot\rho_a(t)$ will play an important role under the condition of strong excitation such as in laser medium or high concentration of active ions. The intensity of the donor fluorescence is proportional to the product of $\rho_d(t)$ and the donor concentration C_d Introducing a coefficient α, the relative intensity of fluorescence is expressed as

$$I(t) = \alpha C_d \rho_d(t) \quad \text{.......} \quad (25)$$

In advance of analyzing an actual fluorescence of a donor-acceptor system, the macroscopic transfer rates corresponding to equations (4) and (5) must be calculated as a function of concentration of donors and acceptors. Förster assumed that the radial distribution function of acceptors around a donor was independent of the acceptor concentration and that the distribution function was proportional to the square of r for all r. These assumptions predicts a linear dependence of the energy transfer rate on the acceptor concentration and a infinite transfer rate at the initial point of decay curves. Although a quadratic dependence of the energy transfer rate was reported [23,24], in addition, the transfer rates are expected to be finite for all the time. In the calculation of macroscopic transfer rates k_{Td} and k_{Ta}, two basic assumptions on the distribution functions for the donors and acceptors were made :

(a) There exists a minimum distance R_n between donors and acceptors.

(b) Donors and acceptors segregate at high concentrations.

This leads to the distribution function for acceptors around a donor,

$$W_a(r) = \begin{cases} 0 & (r < R_n) \\ 4\pi r^2 C_a + 4\pi\beta r^2 C_d C_a \delta(r-R_n) & (r > R_n) \end{cases} \quad \text{,.......} \quad (26)$$

where C_a is the acceptor concentration and β is a coefficient of segregation. These modified distribution of donors and acceptors is shown schematically in Fig.6. The first term $4\pi r^2 C_a$ represents a random distribution outside the sphere of radius R_n The second term $4\pi\beta r^2 C_d C_a \delta(r-R_n)$ represents the segregation of donors and acceptors at the spherical surface with radius R_n. Since the active ions are usually cations, the nearest neighbors must be anions such as O^{2-}. Hence, the distance R_n is expected to be the second nearest neighboring distance for the active ions. With the introduced distribution function, the transfer rate from a donor to acceptors in d-d interaction was obtained as

$$k_{Td} = \frac{4}{3}\pi D k_R \frac{C_a}{R_n^3} + 4\pi D k_R \beta \frac{C_a C_d}{R_n^4} \quad , \text{.......} \quad (27)$$

Same as the function $W_a(r)$, the distribution function of donors around an acceptor was put,

$$W_d(r) = \begin{cases} 0 & (r < R_n) \\ 4\pi r^2 C_d + 4\pi\beta r^2 C_a C_d \delta(r-R_n) & (r > R_n) \end{cases} \quad \text{.......} \quad (28)$$

These distribution functions are shown in Fig.6 Thus the transfer rate for an acceptor is given by

$$k_{Ta} = \frac{4}{3}\pi D k_R \frac{C_d}{R_n^3} + 4\pi D k_R \beta \frac{C_a C_d}{R_n^4} \quad \cdots\cdots (29)$$

These transfer rates k_{Td} and k_{Ta} are finite for all the time and satisfy the quadratic dependence at high concentrations of active ions, as they were expected experimentally.

The fluorescence intensity can be analyzed by the simultaneous calculation of eqs. (24),(25),(29) and (13). A solution in steady state was exactly obtained as as a function of the concentrations of donors and acceptors. In case of transient analysis of fluorescence, the non-linear rate equation was solved numerically for the exact solution was hardly obtained

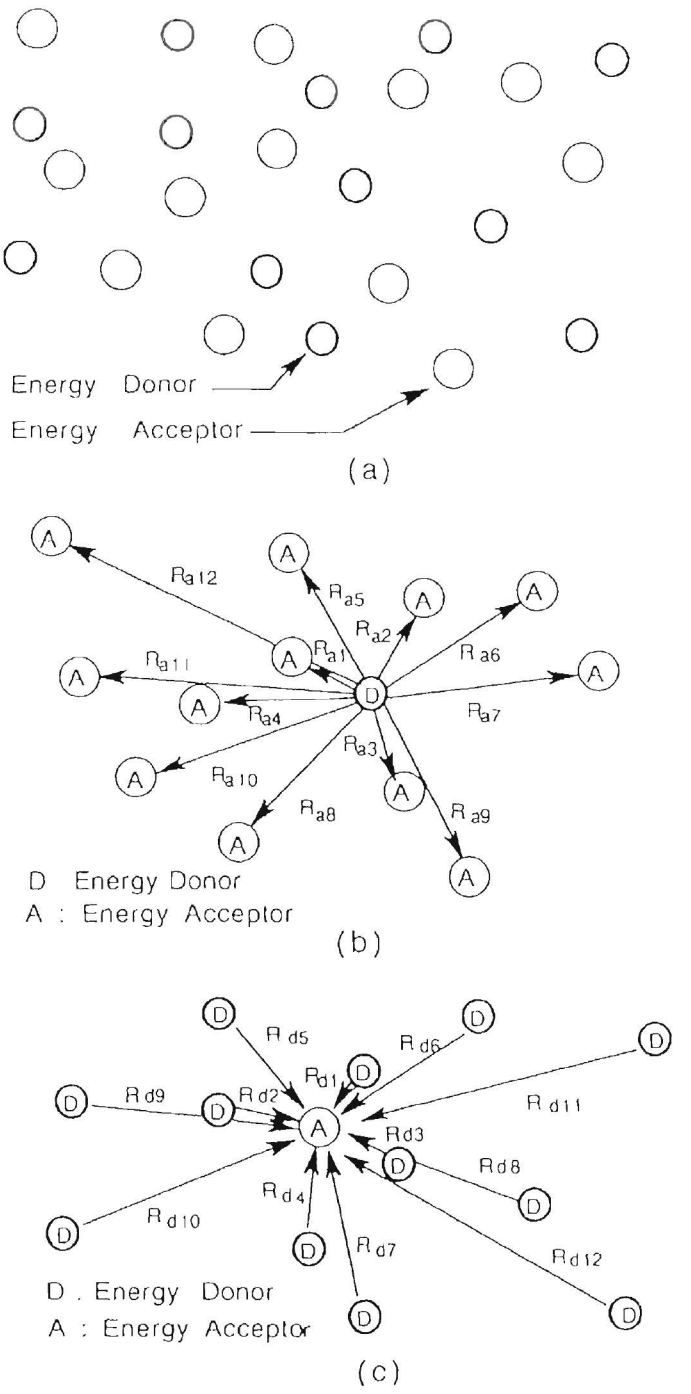

Fig.3 Microscopic model of energy transfer between randomly distributed donors and acceptors. Usually there exist anions such as O^{2} among active ions, although they were omitted in the figure for clarity. A donor gives energy to nearby acceptors and an acceptor obtains energy from nearby donors (a) Spatial distribution of donors and acceptors in glasses. (b) Energy transfer paths from a donor to acceptors. (c) Energy transfer paths from donors to an acceptor.

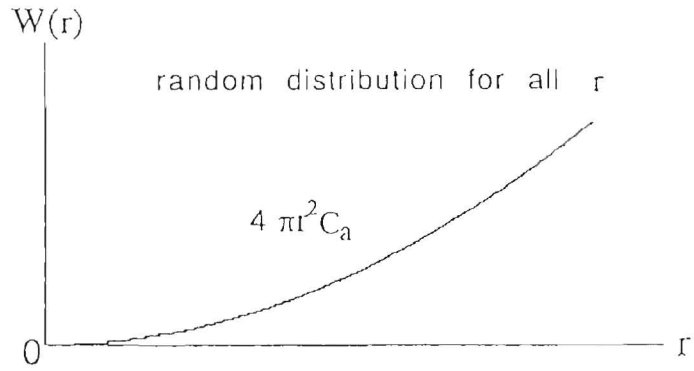

Fig.4. Distribution function of acceptors in the Förster model. The distribution is assumed to be propotional to r^2 even at $r \approx 0$

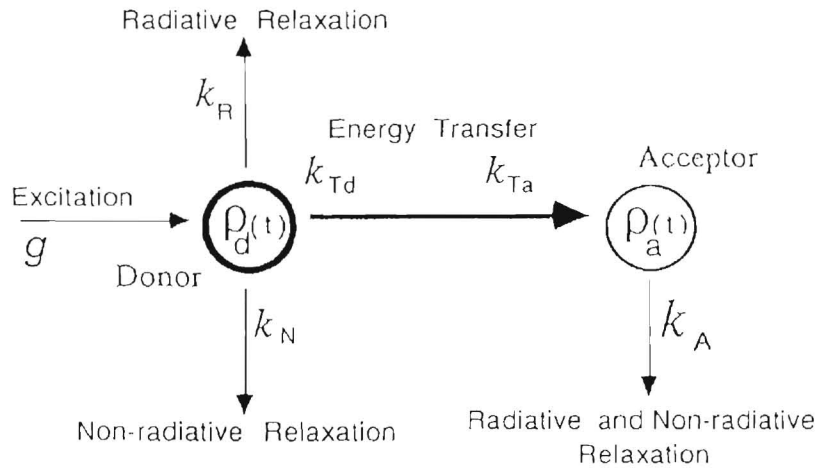

Fig.5. Macroscopic model of excitation , relaxation and transfer of energy. The spatial distributions of donors and acceptors are generally different, therefore these transfer rates k_{Td} and k_{Ta} should be distinguished in the analysis.

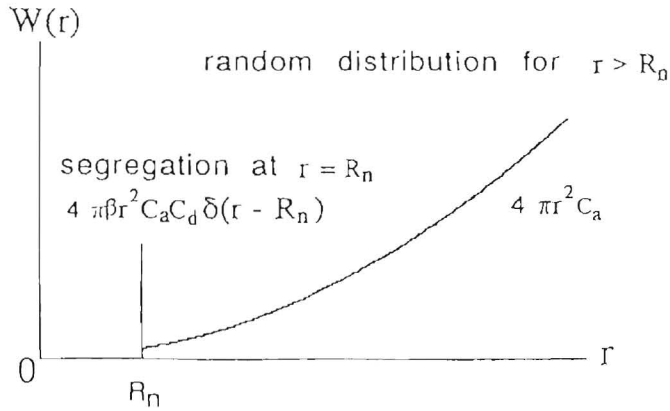

Fig.6. The modified distribution function of acceptors in the non-linear model. The minimum distance R_n between donors and acceptors and the effect of segregation in highly doped conditions are Introduced.

3. Analysis of Experimental results

3.1. Experimental

The glass samples under investigation contained Tb_2O_3 and Na_2O in addition to the network formers (NWF) such as SiO_2, GeO_2, B_2O_3 and P_2O_5. Their compositions are expressed in terms of molar percentages x, y and z as x NWF + y Na_2O + z Tb_2O_3, where $x+y+z=100$ and $y/x=0.5$. The glass samples with $z=0.3$ to 7.0 for each NWF were prepared as listed in table 1. After mixing the raw materials of SiO_2, GeO_2, H_3PO_4, H_3BO_3, Na_2CO_3 and Tb_2O_3 in a clean polyethylene bottle, glass batches were melted for a few hours in a Pt crucible in a furnace at temperatures between 900°C and 1300°C They were then cast and annealed under suitable conditions. Before measuring the fluorescence intensity, all of the glasses were cut and polished in order to ensure the same surface condition

The intensity of the steady-state fluorescence was measured under 360nm wavelength excitation from a mercury lamp at room temperature The apparatus for the measurement consisted of the mercury lamp, band-pass and UV-cutting filters, a monochromator and a photomultiplier . The wavelength-dependent sensitivity of the detection system was calibrated by a standard tungsten lamp The fluorescence of Tb^{3+} under ultra-violet excitation is initiated mainly by electrons at $^5D_3$ and $^5D_4$ levels The fluorescence intensity from the $^5D_4 \rightarrow {}^7F_5$ transition (λ=450 nm) in silicate, phosphate, borate and germanate glasses was measured as a function of Tb_2O_3 concentration, as shown in Fig.7. All measurements were carried out at room temperature. At the lower concentrations than 4 mol% of Tb_2O_3 , the fluorescence intensity of all glasses becomes stronger with increasing Tb_2O_3 content. A slight tendency of the concentration quenching of fluorescence is observed at the higher concentrations. Figure 8 shows the relative fluorescence intensity in steady-state from the the $^5D_3 \rightarrow {}^7F_5$ transition (λ=410 nm) as a function of Tb_2O_3 content with a 360nm wavelength excitation . The quenching of fluorescence with increasing Tb_2O_3 concentration was observed in each of glasses. The fluorescence from the $^5D_3$ state has much stronger tendency of concentration quenching

than that from the $^5D_4$ state. This concentration quenching of the $^5D_3$ fluorescence is recognized as a result of energy transfer from excited Tb^{3+} ions at the $^5D_3$ state to ground state Tb^{3+} ions [31,32].

The fluorescence under ultra-violet excitation originates largely from the $^5D_3$ level when the concentration of Tb^{3+} is low. Since the energy difference between $^5D_3$ and $^5D_4$ levels is equal to that between $^7F_0$ and $^7F_6$, energy transfer can take place between $^5D_3$-$^5D_4$ transition and $^7F_6$-$^7F_0$ transition as illustrated schematically in Fig 9. The energy transfer from $^5D_3$-$^5D_4$ transition to $^7F_6$-$^7F_0$ transition simultaneously generates the energy relaxation from the $^5D_3$ state to the $^5D_4$ state. For this reason it is called $^5D_3$-$^5D_4$ cross-relaxation. This $^5D_3$-$^5D_4$ cross-relaxation becomes important with increasing Tb^{3+} concentration, resulting in the concentration quenching of the of the $^5D_3$ fluorescence and the increase of fluorescence from the $^5D_4$ state. Simultaneous measurements of fluorescence from $^5D_3$ and $^5D_4$ levels are more informative to understand the $^5D_3$-$^5D_4$ cross-relaxation of Tb^{3+} ions. Figure 10 shows the time dependence of Tb^{3+} fluorescence intensity from the $^5D_3$ excited donor state and from the $^5D_4$ metastable state in silicate glasses measured under the N_2-laser excitation. Ground state Tb^{3+} ions are initially excited to the $^5D_3$ state by the pulsed excitation at λ=337nm with the half width of 1ns and then relax by energy transfer or by radiation of a photon. Non-exponential decays, which are the characteristic behavior of the donor fluorescence under the influence of energy transfer, are observed for the $^5D_3$ fluorescence. The intrinsic life-time of the $^5D_3$ fluorescence was evaluated to be 1.0msec. The non-exponential decay of the $^5D_3$ fluorescence and the slow rise of $^5D_4$ fluorescence reflect the population change from $^5D_3$ to $^5D_4$ due to the $^5D_3 \rightarrow {}^5D_4$: $^7F_6 \rightarrow {}^7F_0$ cross-relaxation. The intrinsic life time of the $^5D_4$ fluorescence was measured to be 2.5msec. Thus it is possible to investigate the $^5D_3$-$^5D_4$ cross-relaxation of Tb^{3+} ions by the analysis of the fluorescence intensity originating from the $^5D_3$ level.

3.2. Steady-state analysis

An exact solution in a steady-state can be obtained from the rate equation (24) It is possible to put $k_{Td}=k_{Ta}=k_T$ for the $^5D_3 \rightarrow {}^5D_4$ cross-relaxation between Tb^{3+} ions The equation for ρ_d in a steady-state under a continuous excitation g is

$$k_T(g+k_R+k_N)\rho_d^2+\{k_A(g+k_R+k_N)+k_T(k_A-g)\}\rho_d-gk_A=0 \quad , \quad \cdots\cdots (30)$$

where

$$k_T=k_{Td}=k_{Ta}=\frac{4}{3}\pi R_0^6 k_R \frac{C_d}{R_n^3}+4\pi R_0^6 k_R \beta \frac{C_d^2}{R_n^4} \quad , \quad \cdots\cdots (31)$$

C_d is the concentration of the Tb^{3+} ions and β is a parameter characterizing the segregation of the Tb^{3+} ions. Equation (31) expressing the transfer rate is restricted to the case of d-d interaction. Solving above quadratic equation of ρ_d, one gets the donor population of Tb^{3+} ions as

$$\rho_d(\infty)=\frac{-(k_R+k_N+g)k_A-(k_A-g)k_T+\sqrt{\{(k_R+k_N+g)k_A+(k_A+g)k_T\}^2-4gk_A(k_A+k_T)k_T}}{2k_T(k_R+k_N+g)} \quad , \quad \cdots\cdots (32)$$

The steady state fluorescence from the $^5D_3$ level of Tb^{3+} ions in glasses were analyzed using equation (32) It was determined $k_R=1000\ sec^{-1}$ from the $^5D_3$ decay curves for 0.3mol% of Tb_2O_3. Figure 11 shows the experimental and theoretical results for the fluorescence intensity as a function of the Tb^{3+} ion concentration A quenching of the fluorescence with increasing Tb^{3+} ion concentration is observed for each of the glasses The solid curves are the theoretical results analyzed by the non-linear model with parameters listed in table 2. The non-radiative transition rate k_N was neglected against k_R. These parameters were determined by curve fitting , taking account of the consistency with the following results of time-dependent analysis. Since the non-radiative transition rate increases with increasing dopant concentration, the concentration dependence of k_A was introduced as $k_A=C_{A0}+C_{A1}C_d$. The distance R_n was expected to be 0.4nm, since this is the minimum distance between two Tb^{3+} ions in crystalline Tb_2O_3. The excitation of acceptors is dissipated as phonons or infrared radiation. The multi-phonon process [33,34]

will be dominant for the relaxation from the ^7F_j ($j=0\sim6$) levels of Tb^{3+}. In addition to the cross-relaxation from the $^5D_3 \rightarrow {}^5D_4$ to $^7F_6 \rightarrow {}^7F_0$ transitions, phono-assisted cross-relaxation was reported from the $^5D_3 \rightarrow {}^5D_4$ to $^7F_6 \rightarrow {}^7F_1$ and $^7F_6 \rightarrow {}^7F_2$ transitions [35]. Taking these transitions to the $^7F_0$, $^7F_1$ and $^7F_2$ levels into consideration, the obtained value of $k_A \approx 5 \times 10^3$ at their medium concentration of Tb^{3+} ions corresponds to the report on the energy relaxation by multi-phonon processes [36]. From the experimental results in reference [36], the relaxation rate of acceptors were expected to be $k_A \approx 1 \times 10^4$ in silicate glasses.

Parameters R_0 and β were calculated from the concentration dependence of k_T. The parameters obtained for the Tb^{3+} cross-relaxation and segregation are listed in table 3. The critical transfer distances R_0 were estimated to be 1.0nm~1.1nm. The segregation term $4\pi\beta R_n^2 C_a C_d$, expressing the number of Tb^{3+} ions at the second nearest neighbor position, is in the range 0.4 ~ 5.1 for silicate, phosphate, borate and germanate glasses. The positive values of $4\pi\beta R_n^2 C_a C_d$ indicate the presence of segregation in excess of the average distribution. Judging from these values, the segregation of Tb^{3+} ions in silicate and germanate glasses is stronger than that in borate and phosphate glasses.

3.3. Transient analysis

The decay curves for the donor fluorescence under the influence of the $^5D_3 \rightarrow {}^5D_4$ cross-relaxation were analyzed numerically using the rate equation (24). Figure 12 shows the experimental points of the $^5D_3 \rightarrow {}^7F_5$ emission and the fitted curves by the non-linear analysis in silicate glasses. Non-exponential decays of fluorescence intensity were observed at all contents of Tb_2O_3. The radiative relaxation rate of donors, k_R were determined to be 1.0×10^3 from the $^5D_3$ decay curve for 0.3mol% of Tb_2O_3. The population of acceptors at t=0 and the energy relaxation rate of acceptors were assumed to be

zero in the analysis, namely $\rho_a(0)=0$ and $k_N=0$. The rapid decay of the fluorescence from the $^5D_3$ state with increasing Tb_2O_3 content is due to the cross-relaxation, which transfers electrons from the excited state ($^5D_3$) to the metastable state ($^5D_4$) of the donor ions and excites acceptors. We can neglect the population of the $^5D_4$ metastable state in the analysis, since the $^5D_4$ state has no resonant transitions affecting the cross-relaxation except through the migration or the back-transfer of the excitation. It was estimate by the curve fitting to the experimental results that $\rho_d(0)=0.7$, $R_0^6=3\times10^{-54}m^6$ and $\beta=1\times10^{-36}m^4$ are taken as common parameters for the various Tb_2O_3 contents, assuming electric dipole-dipole interaction. These parameters obtained by the time-dependent analysis correspond to those by the steady-state analysis. Although there found a significant disagreement that the transient analysis gave a much less estimation of the relaxation rate of acceptors than that by the steady-state analysis. The energy relaxation rate of acceptors was estimated to be $k_A<100$ from the transient analysis. It is expected that $k_A\approx1\times10^4$ from experimental results on multi-phonon relaxations mentioned above. Consequently, the energy relaxation rate of acceptors obtained by the steady-state analysis seems to be more reliable than that by the transient analysis. The disagreement in the evaluation of acceptor relaxation between the steady-state analysis and the transient analysis will be mainly due to an effect of energy back-transfer. The effect of energy back-transfer on the fluorescence decays of donors will be discussed later. The migration of energy may be another process causing discrepancy between the theoretical expectations and the experimental results. The migration leading to a macroscopic equilibrium of energy will be important at the initial part of florescence decays.

Next, experimental results for the $Tb^{3+}\rightarrow Nd^{3+}$ energy transfer were examined by means of a numerical calculation. The energy transfer from the $^5D_4\rightarrow{}^7F_4$ transition of Tb^{3+} to the $^4I_{9/2}$ and $^4G_{5/2}$ transition of Nd^{3+} was reported [16]. This process of energy transfer from Tb^{3+} to Nd^{3+} is illustrated schematically in Fig.13. In the analysis, this energy transfer was approximated to a simple system expressed by the rate equation

(24). The fluorescence decay curves were expressed in terms of the Inokuti-Hirayama equation In reference [16]. Figure 14 shows the comparison between the present non-linear analysis and the Inokuti-Hirayama equation for the decay curves of the Tb^{3+} fluorescence in $Ca(PO_3)_2$ glasses under the influence of energy transfer from Tb^{3+} to Nd^{3+}. The curve fit parameters by the non-linear model is listed in table 4 The parameters R_0 and β were estimated as common parameters for the various molar ratios Nd/Tb. The concentration of Tb^{3+} is estimated to be $2\times10^{26}m^{-3}$. The best fit parameters were $R_0^6=1.5\times10^{-54}m^6$ and $\beta=1\times10^{-37}m^4$ for the various concentrations of Nd^{3+} The critical distance was calculated at R_0=1.1nm In this case, the effect of segregation was negligible since $4\pi\beta R_n^2 C_a C_d$ was estimated to be 0.01. It is preferable that one can estimate the parameters k_R, R_0, β, $\rho_d(0)$ and $\rho_a(0)$ to be independent of the rations Nd/Tb. We can also find that both the non-linear model and the Inokuti-Hirayama equation give good fittings to the experimental results of donor fluorescence It was a surprise that these two analyses give similar decay curves in the time region longer than the relaxation time of the system. However, it should be noted that the decay curves predicted from the Inokuti-Hirayama equation are non-exponential in its nature, even at low acceptor concentration, and that the first derivative of the Inokuti-Hirayama equation becomes infinite at $t = 0$. In order to examine the differences between these models, decay curves predicted from them were compared in a very short time range, as shown Fig 15. The decay curves predicted from the non-linear analysis become exponential near the initial point, yielding a reasonable energy transfer rate at $t \approx 0$ Experimental results on the donor fluorescence supports single-exponential decays as a short time response just after a pulsed excitation.

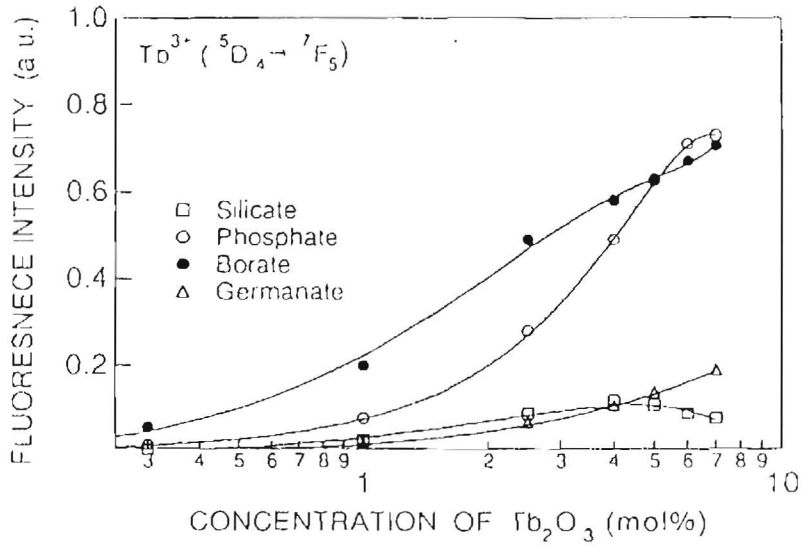

Fig.7. Fluorescence intensity in steady-state from the $^5D_4$ level of Tb^{3+} ions

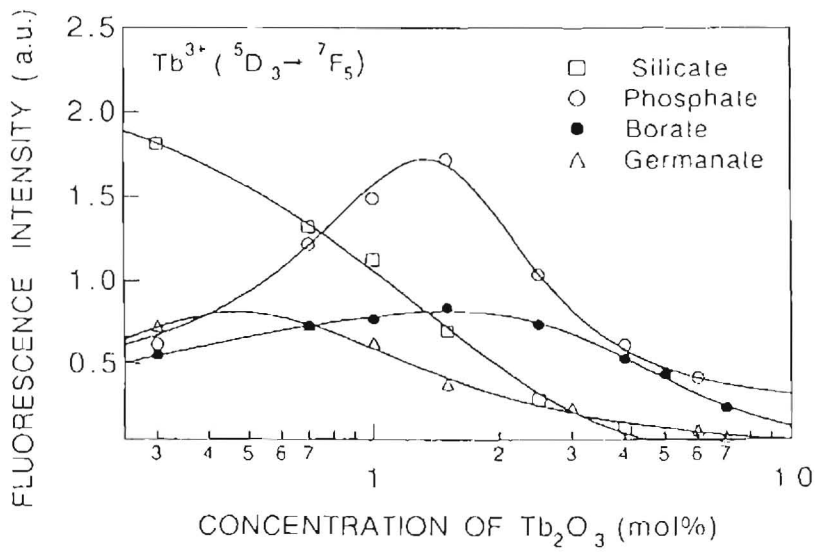

Fig.8 Fluorescence intensity in steady-state from the $^5D_3$ level of Tb^{3+} ions. The quenching of the fluorescence with increasing Tb_2O_3 concentration was observed in all glasses.

Table 1 Sample data of Tb^{3+}-doped glasses.

NWF	SiO_2	GeO_2	B_2O_3	P_2O_5
Base glass composition (mol%)	$67SiO_2+33Na_2O$	$67GeO_2+33Na_2O$	$67B_2O_3+33Na_2O$	$67P_2O_5+33Na_2O$
Sample composition (mol%)	x NWF + y Na_2O + z Tb_2O_3 ($x + y + z = 100$, $y/x = 0.5$)			
Doped Tb_2O_3 (mol%)	z = 0.3, 0.7, 1.0, 1.5, 2.5, 4.0, 6.0 and 7.0			
Melting temperature	1300 °C	1000 °C	1200 °C	900 °C
Annealing	400~100 °C	450~100 °C	450~100 °C	200~100 °C
	- 20 °C / hour			
Size	5 mm X 5 mm X 8 mm			

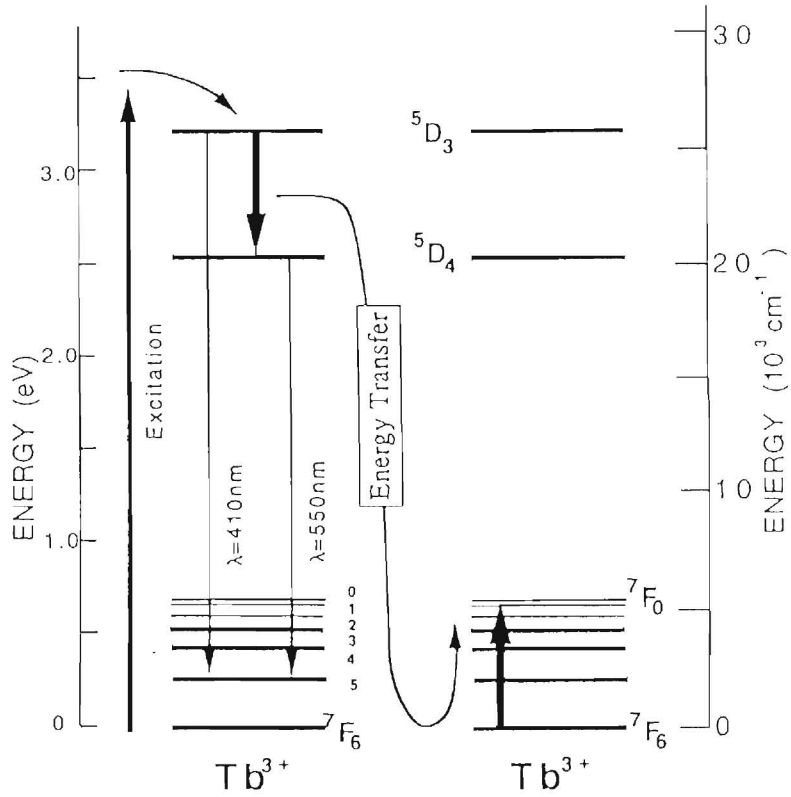

Fig 9. Simplified energy levels of Tb^{3+} ions Thick arrows illustrate the $^5D_3$-$^5D_4$ cross-relaxation between neighboring Tb^{3+} ions

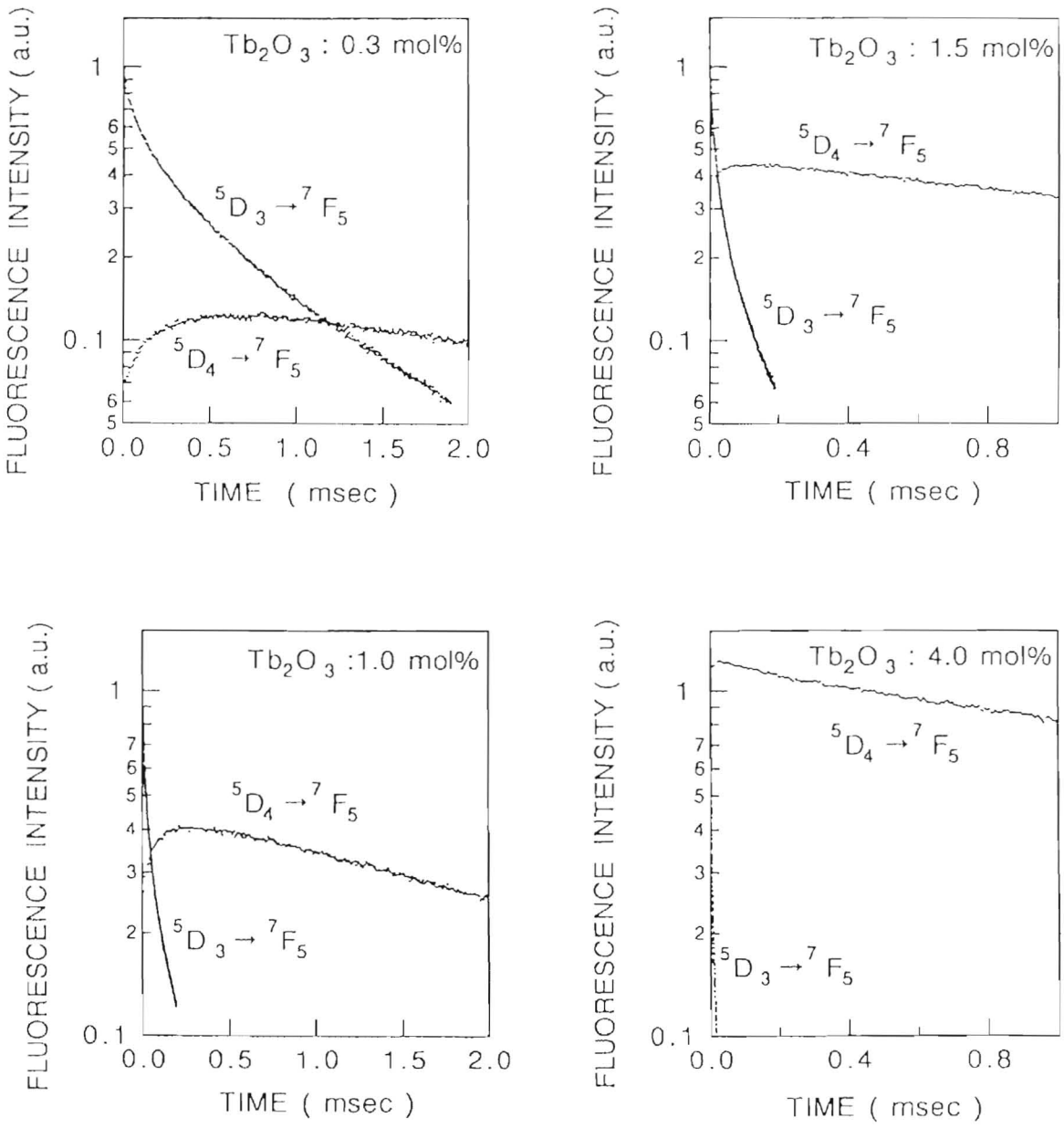

Fig.10. Fluorescence decay curves from the $^5D_3$ (donor) level and the $^5D_4$ level of Tb^{3+} in a silicate glass. The non-exponential decay of the $^5D_3$ fluorescence and the slow rise of the $^5D_4$ fluorescence reflect the energy transfer from the $^5D_3$ level to the $^5D_4$ level.

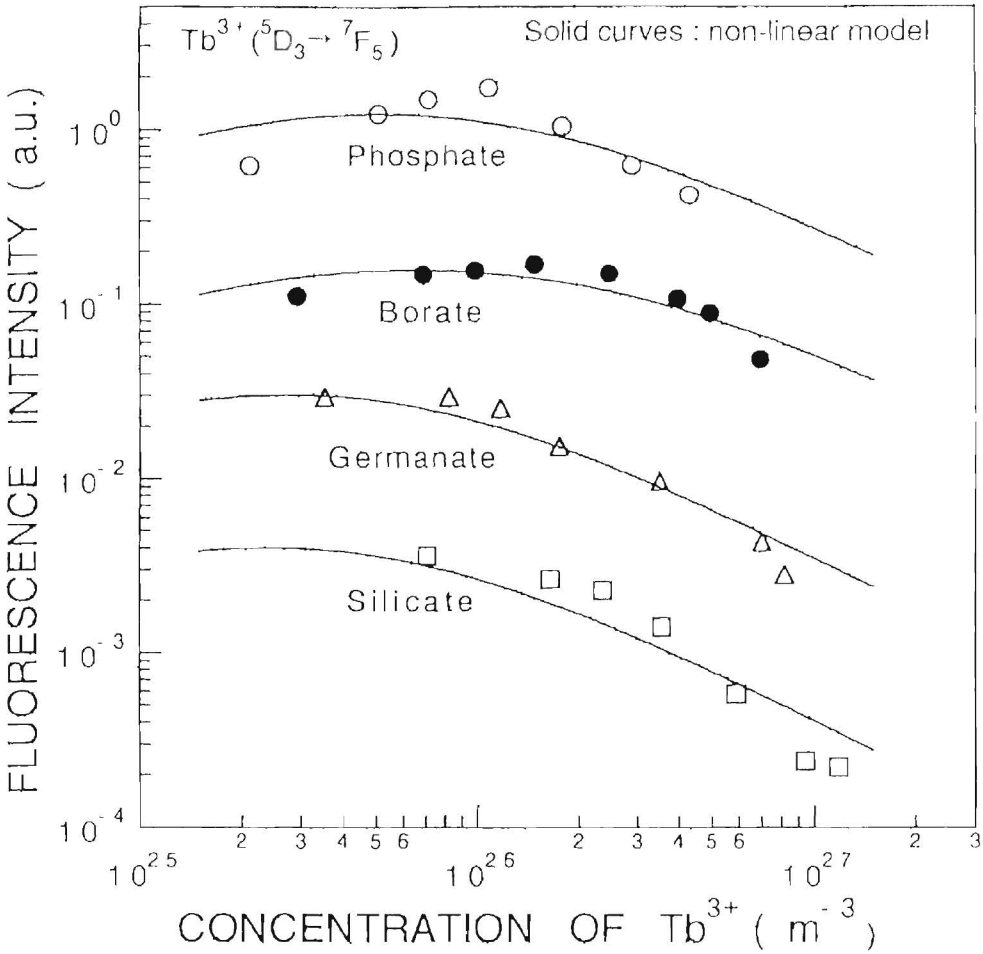

Fig.11. Steady-state fluorescence intensity for the $^5D_3$ level of Tb^{3+} with the origins displaced for clarity. The quenching of the fluorescence with increasing Tb_2O_3 concentration was observed in all glasses.

Table 2. Curve fit parameters of Tb^{3+}-Tb^{3+} energy transfer in steady-state .

Host Glass	Silicate	Phosphate	Germanate	Borate
k_R (sec^{-1})	$1x10^3$	$1x10^3$	$1x10^3$	$1x10^3$
k_{A0} (sec^{-1})	70	56	117	53
k_{A1} ($sec^{-1}\ m^3$)	$3.5x10^{-26}$	$1.2x10^{-25}$	$1.5x10^{-25}$	$1.8x10^{-26}$
R_0^6 (m^6)	$6.7x10^{-54}$	$6.3x10^{-54}$	$3.4x10^{-54}$	$3.7x10^{-54}$
α	$3.1x10^{-24}$	$1.4x10^{-24}$	$1.3x10^{-24}$	$1.3x10^{-24}$
β (m^4)	$1.4x10^{-36}$	$2.4x10^{-37}$	$1.5x10^{-36}$	$6.3x10^{-37}$
g (sec^{-1})	69	72	91	50

k_R : radiative transition rate of donors .

$k_A = k_{A0} + C_{Tb}\, k_{A1}$: energy relaxation rate of acceptors .

$$R_0^6 = \frac{3\hbar^4 c^4}{4\pi n^4}\left(\frac{\varepsilon}{\kappa^{1/2}\varepsilon_c}\right)^4 \int \sigma_a(E)dE \int \frac{f_d(E)\, f_a(E)}{E^4} dE$$

α : a coefficient .

β : a coefficient characterizing the segregation .

g : excitation rate of donors .

Table 3 Parameters of cross-relaxation and segregation.

Host Glass	R_0 (nm)	$4\pi\beta R_n^2 C_a C_d$
Silicate	1.37	3.4
Phosphate	1.36	0.1
Germanate	1.23	2.0
Borate	1.24	0.6

R_0 : critical distance of energy transfer.

$4\pi\beta R_n^2 C_a C_d$: the number of the condensed Tb^{3+} ions at the second nearest neighbouring position.

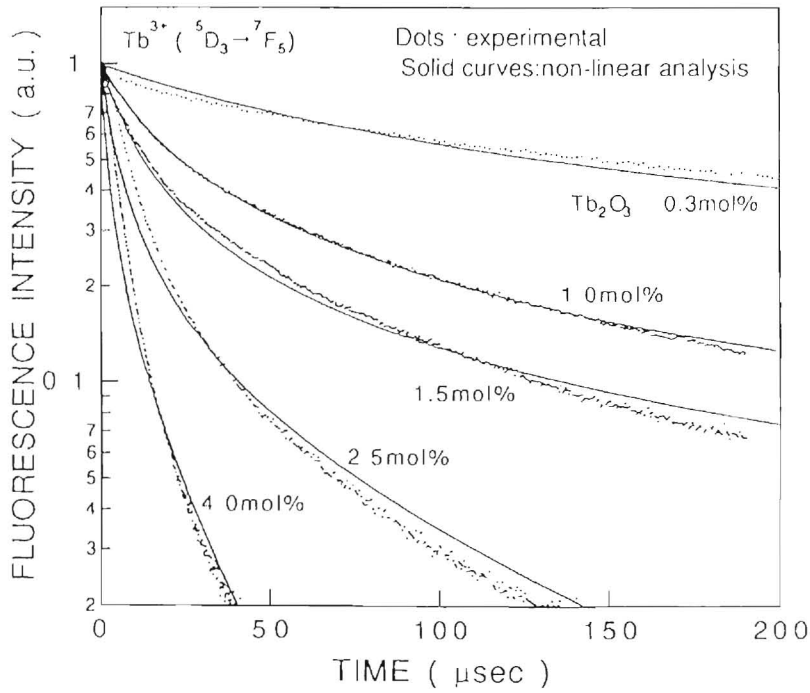

Fig.12. Decay curves of donor fluorescence under the influence of the $^5D_3$-$^5D_4$ cross-relaxation. Theoretical curves (solid curves) were fitted to the experimental results (dots).

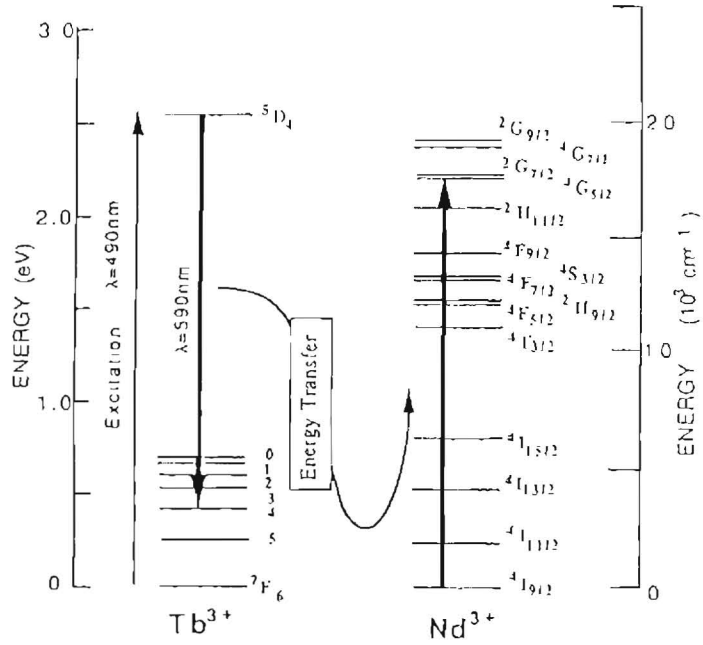

Fig.13. Schematic energy levels of Tb^{3+} and Nd^{3+} ions. Thick arrows illustrate energy transfer from Tb^{3+} to Nd^{3+} ions.

Table4. Curve fit parameters for the Tb^{3+}-Nd^{3+} energy transfer. Parameters k_R, R_0, β, $\rho_d(0)$ and $\rho_a(0)$ were determined to be independent of the rations Nd/Tb.

Molar Ratio	Nd/Tb = 0.0	Nd/Tb = 0.2	Nd/Tb = 0.5	Nd/Tb = 1.0
k_R (sec^{-1})	400	400	400	400
k_N (sec^{-1})	32	109	227	293
k_A (sec^{-1})	0	5	5	5
k_{Td} (sec^{-1})	0	2.4×10^3	6.0×10^3	1.2×10^4
ρ_d (t = 0)	1.0	1.0	1.0	1.0
ρ_a (t = 0)	0.0	0.0	0.1	0.25
C_a (m^{-3})	0.0	4×10^{25}	1×10^{26}	2×10^{26}
R_0^6 (m^6)	———	2×10^{-54}	2×10^{-54}	2×10^{-54}
β (m^4)	———	1×10^{-37}	1×10^{-37}	1×10^{-37}

k_R : radiative transition rate of donors.
k_N : non-radiative transition rate of donors.
k_A : energy relaxation rate of acceptors.
k_{Td} : energy transfer rate from a donor to acceptors.
C_a : concentration of acceptors.
β : a coefficient characterizing the segregation.

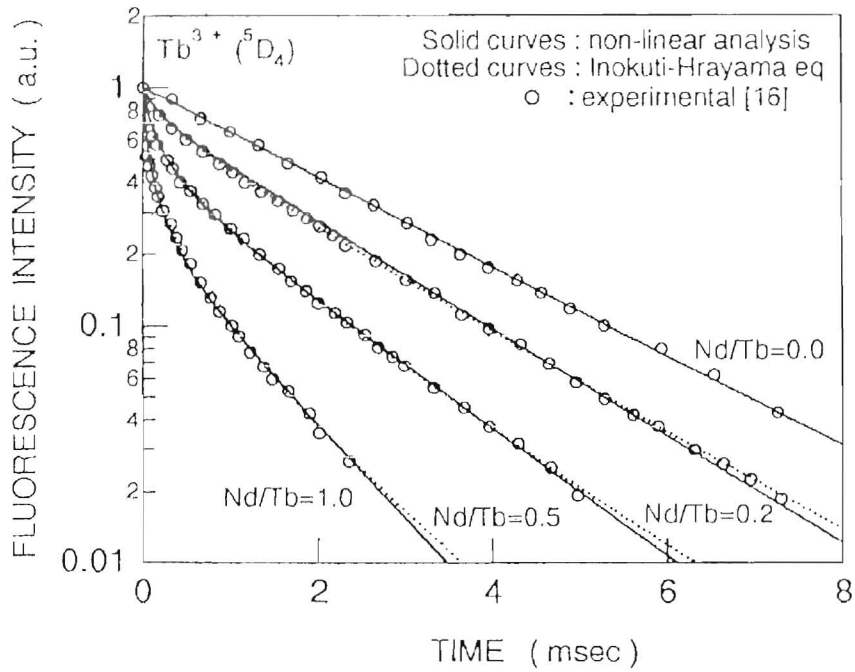

Fig.14. Fluorescence decay curves for Tb^{3+} ions under the influence of energy transfer to Nd^{3+} in $Ca(PO_3)_2$ glasses. The theoretical curves by the non-linear model (solid curves) and by the Inokuti-Hirayama eqation (dashed curves) were fitted to the experimental data.

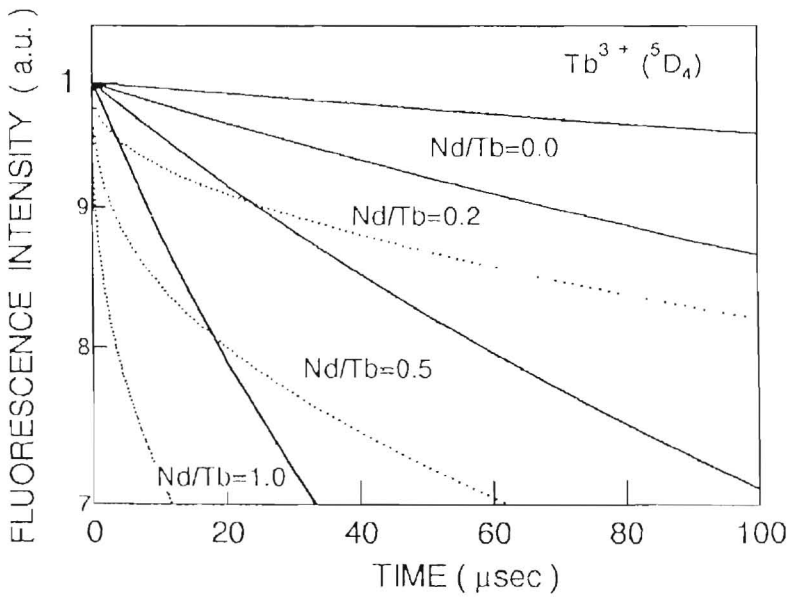

Fig.15. Comparision of decay curves predicted by the non-linear model and the Inokuti-Hirayama equation. The decay curves by the Inokuti-Hirayama eq. become very steep near the initial point even at low acceptor concentration. On the contrary, the decay curves by the non-linear analysis become exponential near the initial point, yielding a reasonable energy transfer rate at t≈0. Experimental results at t≈0 supprorts the exponential behavior of donor fluorescence.

4. Stochastic model

4.1. Stochastic rate equations

In previous models, energy transfer were analyzed by rate equations for the averaged populations of donors and acceptors. However these averaged populations, $\rho_d(t)$ and $\rho_a(t)$, might be inadequate to represent the status of the system. Since the transfer of energy induced mainly by multi-polar interaction effective only in a short distance, the local distribution of acceptors around the excited donor will be dominant for the dynamics of energy transfer. Thus the consideration of local distribution of excitations is preferable for more accurate analysis of energy transfer. This consideration of individual excitations on donors and acceptors will be performed by discriminating all active ions and by quantizing energy associated with all transitions. The idea of energy quantization is applied to the analysis of energy transfer for the first time. Most models including the non-linear model and the Förster model, have never satisfied the discrete property of energy, since the analyses were based on the infinitesimal flow of energy in those models. As a result of quantization of energy, all transitions should be stochastically calculated. It is appropriate to build a new model for energy transfer based on the elementary process of pair-transfer, considering the discrimination of all active ions and the quantization of transferred energy [41].

The time development for the excitations of the i-th donor and the j-th acceptor at $t+\Delta t$ is given by the following equation,

$$\begin{cases} \rho_{di}(t+\Delta t) = \Delta t\, g(1-\rho_{di}(t)) - \sum_{j=1}^{Na} k_T(r_{ij})\,\Delta t\,\rho_{di}(t)\,(1-\rho_{aj}(t)) - (k_R+k_N)\,\Delta t\,\rho_{di}(t), & i=1 \sim Nd \\ \rho_{aj}(t+\Delta t) = \sum_{i=1}^{Nd} k_T(r_{ij})\,\Delta t\,\rho_{di}(t)\,(1-\rho_{aj}(t)) - k_A\,\Delta t\,\rho_{aj}(t), & j=1 \sim Na \end{cases} \quad \cdots\cdots\cdots\cdots (33)$$

where Δt is a small step of time, g is the excitation rate of donors, N_a is the number of acceptors, N_d is the number of donors, $k_T(r_{ij})$ is the energy transfer rate from a donor to the acceptor at the distance of r_{ij}, k_R is the radiative transition rate of donors, k_N is the

non-radiative transition rate of donors, and k_A is the energy relaxation rate of acceptors. Since this is an stochastic approach, the time dependence of the excitations of donors and acceptors should be formalized in a difference equation. All possible transfer paths from excited donors to ground state acceptors are explicitly explained in equation (33) using two-body expansion. Unlike most models, the excitation and the transferred energy is quantized in this model. Hence, the population of donors and acceptors must be equal to 0 or 1. Namely, $\rho_{di}(t)=0,1$ and $\rho_{aj}(t)=0,1$ for all i and j. These conditions of the transitions are quite reasonable from the quantum mechanical point of view. The schematic flow of energy for a donor-acceptor pair is shown in Fig.16. Donors are excited at the first step. Then they relax their excitations radiatively or non-radiatively, or simultaneously transfer some energy to acceptors. That the energy transfer is mostly a two-body process, allows to use the two-body expansion for the modeling of the complex donor-acceptors system.

It is informative to compare the non-linear model, the Förster model and the stochastic model in a form of rate equation. The rate equation for the stochastic model can be given as

$$\begin{cases} \dfrac{d\rho_{di}(t)}{dt} = g(1-\rho_{di}(t)) - \displaystyle\sum_{j=1}^{Na} k_T(r_{ij})\,\rho_{di}(t)\,(1-\rho_{aj}(t)) - (k_R+k_N)\,\rho_{di}(t), \quad i=1\sim Nd \\ \dfrac{d\rho_{aj}(t)}{dt} = \displaystyle\sum_{i=1}^{Nd} k_T(r_{ij})\,\rho_{di}(t)\,(1-\rho_{aj}(t)) - k_A\,\rho_{aj}(t), \quad j=1\sim Na \end{cases} \qquad \cdots\cdots(34)$$

This expression in a rate equation might lose the exactness of the stochastic model. However, we can easily understand this coupled equation as an extension of the non-linear model, comparing with the rate equation (24). Equation (34) can be recognized also as an extension of the Förster's rate equation. It is still important that equation (34) is stochastic rate equation. Migrations, diffusions and back transfer of energy are neglected here for simplicity.

4.2. Analysis of experimental data by Monte Carlo simulations

Experimental results for the $Tb^{3+} \rightarrow Nd^{3+}$ energy transfer [16] were numerically analyzed by means of a computer simulation based on eq (33). In the calculation, 3200 excited donors and 12800 ground state acceptors were randomly generated as the initial condition. The radiative transition of donors, the energy transfer from donors to acceptors within the pair-distance of 3nm, and the energy relaxation of acceptors were stochastically calculated step by step . The energy moves from the excited donor mostly to its nearest acceptor . Transfer of energy to farther acceptors will be negligible small for an actual system. Consequently, the cutoff at 3nm in the calculation of energy transfer is considered enough due to the short critical transfer distance about 1.4nm. However, the energy transfer for all probable combinations of donors and acceptors is expected to be evaluated. The The dependence of the transfer probability on the distance is r^{-6}, r^{-8}, r^{-10} for d-d , d-q and q-q interactions, respectively. The generation rate, g was supposed to be zero for the decay curves just after a pulsed excitation.

Simulated curves for the d-d, the d-q and the q-q interactions, were fitted to the experimental points of the donor fluorescence, as shown in Fig.17. The energy transfer is from the $^5D_4 \rightarrow {}^7F_4$ transition of Tb^{3+} ions to the $^4I_{9/2} \rightarrow {}^4G_{5/2}$ transitions of Nd^{3+} ions. The radiative transition rate of donors k_R was determined at $430sec^{-1}$ by a single exponential fit to the experimental points of Nd/Tb=0. The critical transfer distance, R_0 was evaluated in stead of the function $k_T(r_{ij})$. The function $k_T(r)$ was assumed in the form,

$$k_T(r) = k_R \left(\frac{R_0}{r} \right)^s \qquad \cdots\cdots (35)$$

Parameters k_A and R_0 listed in Table 5 were determined to give the best fits in a long time range. A definite value of k_A is obtained only on the assumption of d-q interaction Figure 18 shows the behavior in a short time range given by another trial of calculation with the same set of parameters. It is clarified that the results of the calculation supposing q-q interactions changed too much with time and that of d-d interactions, too little The decay

curves of d-q interaction (r^8) seems the best fit to explain the experimental data in the whole time range between 10μs and 1ms. Figure 19 shows the histogram to clarify the deviations of the calculations from the experimental data for 100 trials of d-d, d-q and q-q interaction models, respectively. It is evident that d-q interactions fit best among those.

The validity of the stochastic model was examined by comparing the parameter k_A with other experimental results. We examined the obtained parameter k_A by comparing with other experimental results. It is known that the Nd^{3+} ions excited at the $^4G_{5/2}$ state relax to their ground state mainly via the $^4F_{3/2}$ state. From some experimental results [42,43], the parameter k_A was estimated to be about $2x10^3 sec^{-1}$, which include the life time at the $^4F_{3/2}$ state. It was found that the obtained value k_A=370sec^{-1} by our Monte Carlo simulation was much smaller that that by experiments. This underestimation of the relaxation rate of acceptors will be brought by the neglects of energy back-transfer. The analysis without considering the back-transfer of excitation will commonly give an underestimated rate of energy relaxation for acceptors. Since the pair of the excited acceptor and the ground state donor is always generated as a result of the energy transfer in the forward direction, some excitations of acceptors will go back to the donors nearby. Thus the net transfer of energy from donors to acceptors is reduced by the presence of energy back-transfer. A better agreement will be obtained by an analysis considering the back transfer processes. An extended calculation considering the back-transfer processes, will be carried out in the next chapter. The Monte Carlo technique used here is proved effective to calculate the complex interaction processes of the energy transfer kinetics and to evaluate the additional effects of migrations and/or back-transfers.

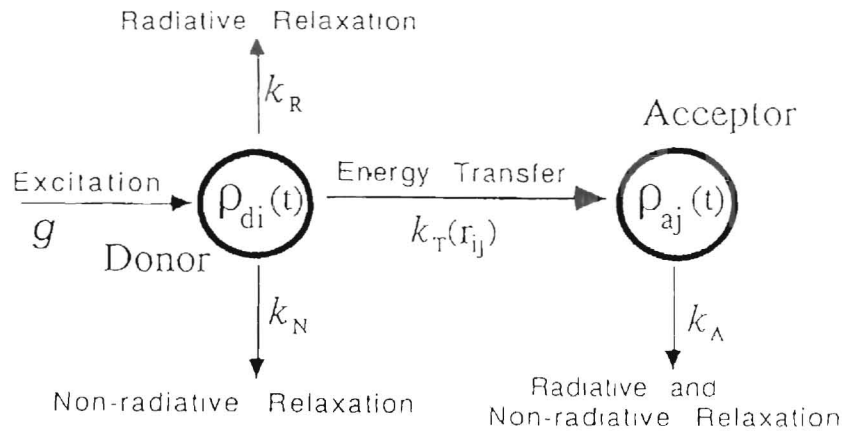

Fig.16. Microscopic model of energy transfer

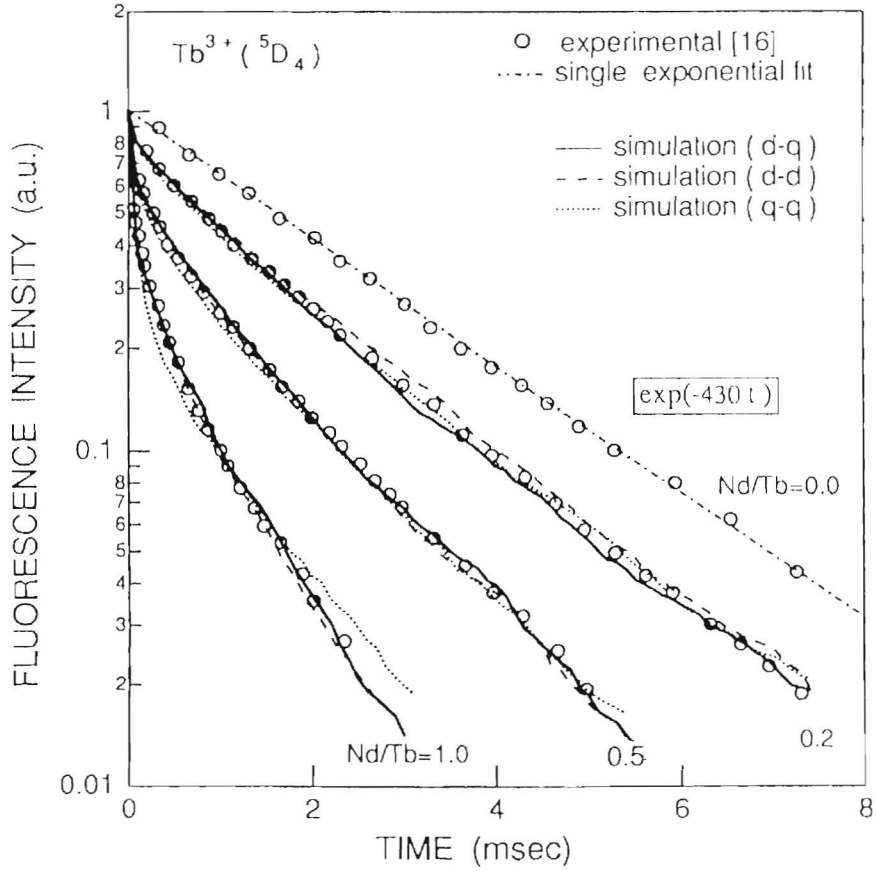

Fig.17. Decay curves of donor fluorescence in a long time range. Simulated curves for the d-d, the d-q and the q-q interactions, were fitted to the experimental points.

Table 5 Obtained arameters of best fit curves for the energy transfer from Tb^{3+} to Nd^{3+} ions determined by the stochastic model.

interaction	d - d	d - q	q - q
dependence on r	-6	-8	-10
k_n (sec^{-1})	430	430	430
k_A (sec^{-1})	< 20	370±40	> 5000
R_o (nm)	1.39	1.36	1.30

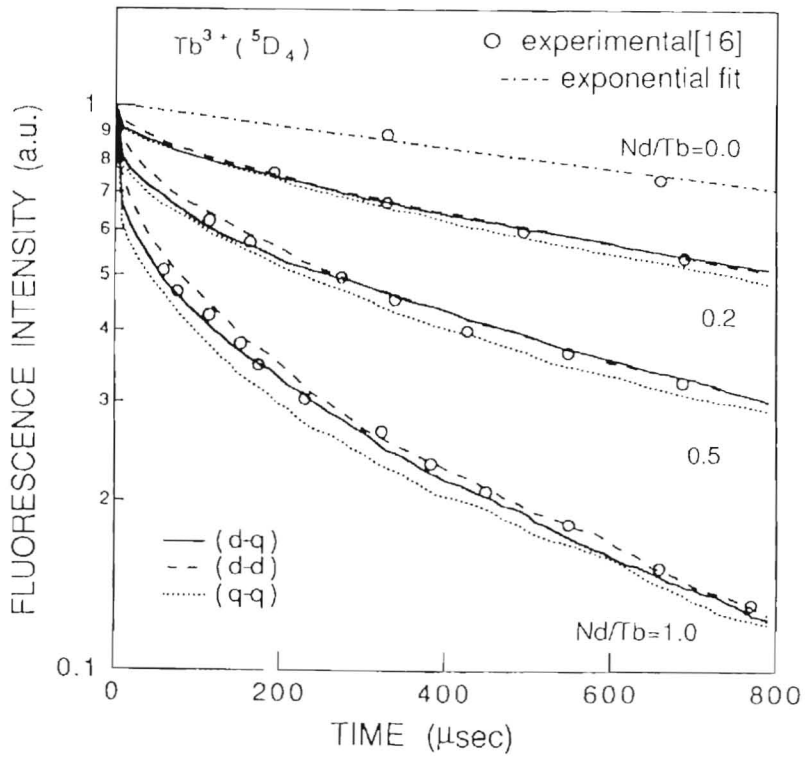

Fig.18. Decay curves of donor fluorescence in a short time range. The decay curves of d-q interaction seems the best fit to explain the experimental data.

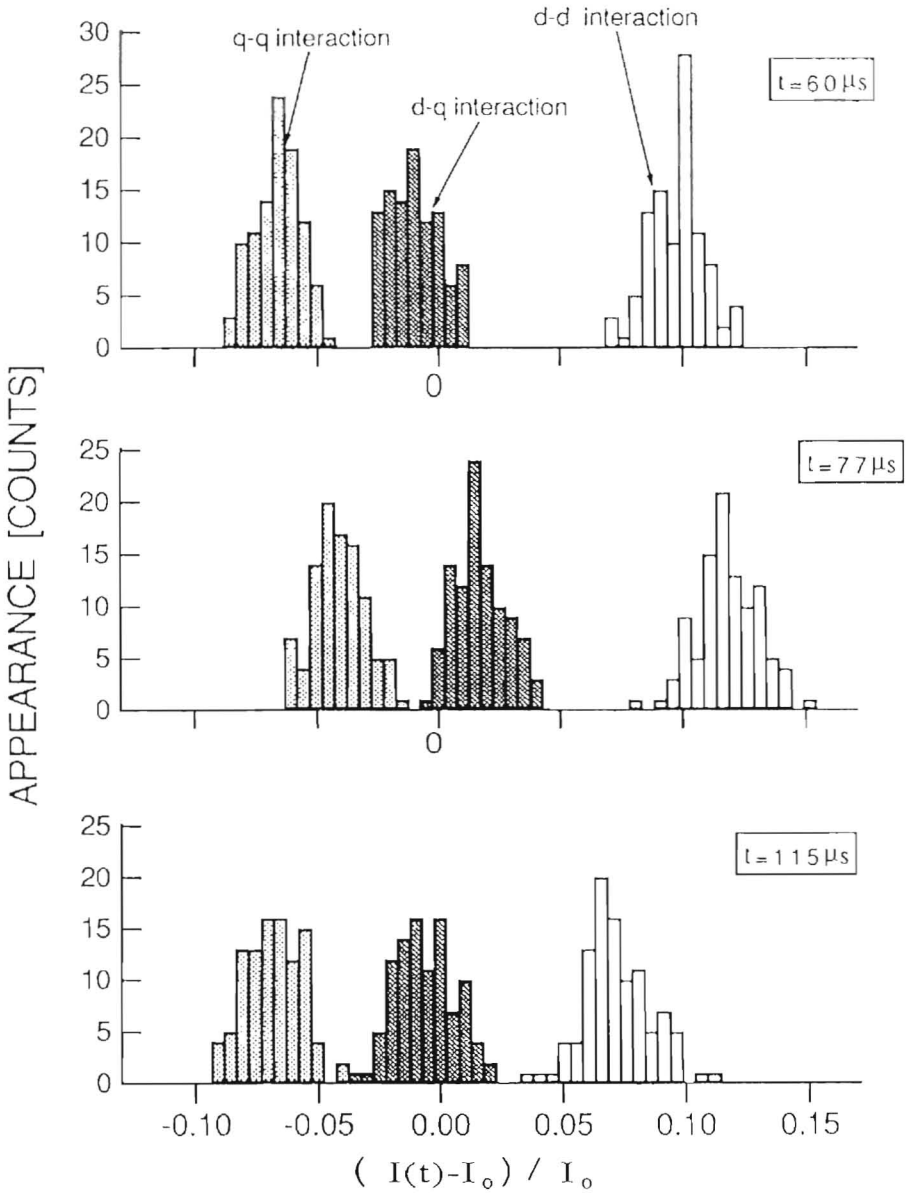

Fig.19. Deviations of simulated results from the experimental points. Calculations were carried out for d-d, d-q and q-q interaction models with 100 trials, respectively. It is evident that the d-q interaction model fits best among those.

5. Discussions

5.1. Origins of non-exponential responses

Phenomenological agreements between experimental results on the decay curves of donor fluorescence and predictions by the Inokuti-Hirayama equation were often reported, however, some difficulties with the Förster-like models were also pointed out. These difficulties such as the infinite energy transfer rate at the initial point of decay curves and the inability to analyze steady-states seem to be serious to the theoretical consistency of all Förster-like models. In the non-linear model, the non-exponential responses were found to be caused by the non-linearity of the rate equation. From a mathematical point of view, it is quite reasonable to understand the non-exponential decays as a result of the non-linearity in the rate equation. On the other hand, the mathematical origin of the non-exponential decay in the Förster model are not clear for its complex mathematical treatments. Our main question to the Förster-like models is the theoretical consistency in getting the non-exponential decay function from a linear rate equation. The exact solutions of a linear rate equation of first order must be single-exponential functions from a mathematical requirement. We recognize that the Förster model gives good fits to experimental results. Actually, the Inokuti-Hirayama equation have been most widely used for the analysis of donor fluorescence. This usefulness of the Förster model will mean that it gives a good approximation to the decay functions of donor fluorescence in some conditions. And yet, limitations to the Förster model are also unclear for its complicated procedures obtaining the macroscopic response of the donor fluorescence. Therefore it is still worthwhile to investigate the steps leading to the non-exponential function after treatments by Förster and Inokuti-Hirayama. Since all of these models can give good fits to experimental results, one can hardly find out the best model from phenomenological investigations. Thus, these models should be examined especially concerning on the theoretical consistency.

The treatments in the Förster model were studied from a theoretical point of view. Equation (1) is an acceptable equation for the donor population when the population of acceptors is neglected. Equations (2) and (3) are exact solutions of eq. (1). It should be noticed that eq.(3) is not a exact solution but an approximated one. The exact formula should be

$$\overline{\rho(t)} = \rho(0)\exp(-k_R t)\ \exp\{-k_R \lim_{R_g\to\infty} \int_0^{R_g} N\, w(r)\ (\frac{R_0}{r})^s dr\ t\} \quad \cdots\cdots (36)$$

since the function w(r) describes the the distribution of distance r. We can find that the function $\overline{\rho_d(t)}$ is still single-exponential from eq. (34) even with the introduction of distribution function w(r) . It is quite natural to be single-exponential from a mathematical point of view On the other hand, the function $\overline{\rho_d(t)}$ given by eq. (4) is already non-exponential. The non-exponentiality of eq. (4) might not be clear. It is helpful to examine the case of discrete distribution of acceptors. For a special case of w(r), eq (4) becomes

$$\overline{\rho(t)} = \rho_0\exp(-k_R t)\ [N_1\exp\{-k_R(\frac{R_0}{r_1})^s t\} + N_2\exp\{-k_R(\frac{R_0}{r_2})^s t\}]^{N_1+N_2} \quad \cdots\cdots (37)$$

where the number of distributed acceptors are assumed to be N_1 at $r=r_1$ and N_2 at $r=r_2$ It is apparent that the function $\overline{\rho_d(t)}$ defined by eq. (35) consists of a linear combination and non-linear products of single-exponential functions. Thus the decay function (4) is non-exponential. Reconsidering the transformation from eq. (3) to eq.(4), we find that the eq. (4) is an approximation and that the non-exponential decays arise from eq. (4). Therefore it can be concluded that the origin of non-exponential decays in the Förster model is due to the approximation of the exact solution to eq.(4). Such approximation required to obtain the decay function seems to be fatal to the theoretical consistency of the Förster model. There might be another possibility to remedy the Förster model. The main objective against our interpretations will be that the original equation (1) is incorrect and that the correct function is given by eq.(4). However, the exact rate equation for eq.(4) has not been found yet The proper approach for the theoretical study of donor fluorescence should begin with the formalization of a rate equation for the system. Since no rate equation from which eq.(4) is given as an exact solution has been found in spite of mathematical investigations, I am negative to eq. (4) as a theoretical function for the donor fluorescence under the influence of energy transfer.

Next question to be discussed in this chapter is what is the appropriate rate equation for the non-exponential properties of the donor fluorescence. The basic physical picture of energy transfer will be the following processes:

(1) Energy transfer occurs from excited donors to ground state acceptors.

(2) The acceptor obtained energy will stay excited during its life time.

(3) The deexcited donors and excited acceptors give no influence on the dynamics of energy transfer.

(4) The elementary process of energy transfer is a exchange of excitation between a donor and an acceptor.

(5) Only one excitation is exchanged between a donor and an acceptor at a time.

In addition, it will be widely accepted that the pair-transfer function derived by the perturbation method is applicable also to the complex interactions between many donors and acceptors. All of these conditions were well formalized only in the stochastic model. Therefor, the rate equation (17) by the stochastic model is most acceptable. It is clear from eq. (16) and (17) that the non-linearity related to the excitation of donors and acceptors is the point to generate non-exponential decays. We can also derive the Förster model by introducing the averaged population of excited ions and by reducing the non-linear rate equation to a linear form. The non-linearity had been regarded low enough in average. Although, it seems to be the most important effect for the dynamics of energy transfer. Since the energy transfer occurs from a donor mainly to its nearest acceptor, the non-linearity will be locally enhanced in the neighborhood of the excited ion. Thus the non-linear effect is expected to appear stronger than it had been believed. Consequently, the non-linear effect associated with the excitation donors and acceptors has found to be the most acceptable origin to the non-exponential decays of donor fluorescence.

5.2. Effect of energy back-transfer

The last process considered is the back-transfer of energy. In this chapter, the fluorescence of Tb^{3+} ions in glasses was analyzed by the non-linear model considering a back-transfer process. While there were a few reports on the back-transfer of electronic excitation [54,55], no correspondence with the experimental results has been examined. Once the energy transfer from a donor to an acceptor has occurred, there exist the excited acceptor and the ground-state donor in a distance enough to interact. Thus the energy of the excited acceptor can go back to the ground-state donor nearby. From the basic formula by Förster and Dexter , energy transfer

rate strongly depends on the overlap of emission and absorption spectra. Since the Stokes shift of rare-earth ions is small, the increased overlap integral will lead to an enhancement of the back-transfer. Furthermore, phonons at room temperature [51] and the spectral broadening characteristic of glasses will increase the transfer rate in both directions As a consequence, not only the forward-transfer but also the back-transfer will play an important role in the energy transfer process. Roughly speaking , the Stokes shift of Tb^{3+} is same as the half width of the emission lineshape from some experimental results [52,53]. They are typically about 10nm in a silicate glass, hence we can estimate the efficiency of the back-transfer as η_B=0.2, assuming that the normalized emission spectrum of donors and the normalized absorption spectrum of acceptors are equal and that that these lineshapes of emission and absorption are Gaussian , as shown in fig.20. The back-transfer rate of energy will be proportional to the acceptor population in excited state and the donor population in ground state .

Introducing the population of acceptors, the excitation term and the back-transfer of energy, we begin with the following rate equation for the population of donors and acceptors in excited state under the influence of energy transfer.

$$\begin{cases} \dfrac{d\rho_d(t)}{dt} = (1-\rho_d(t))\,g - (k_R + k_N)\rho_d(t) - k_{Td}(1-\rho_a(t))\rho_d(t) + \eta_B k_{Td}\rho_a(t)(1-\rho_d(t)) \\ \dfrac{d\rho_a(t)}{dt} = k_{Ta}(1-\rho_a(t))\,\rho_d(t) - \eta_B k_{Ta}\rho_a(t)(1-\rho_d(t)) - k_A\rho_a(t) \end{cases} , \quad \cdots\cdots\cdots (38)$$

where k_N is the non-radiative transition rate of donors, k_A is the energy relaxation rate of acceptors, k_{Td} is the energy transfer rate from a donor to acceptors, k_{Ta} is the energy transfer rate from donors to an acceptor , η_B is the efficiency of the back-transfer and g is the excitation rate of donors. It was difficult for the Förster and Inokuti-Hirayama models to include the back transfer of energy for its disregarding of acceptor excitation.

It is possible to analyze the donor fluorescence with the effect of back transfer in a simple case using the rate equation (36). For the fluorescence of Tb^{3+} ions, the life time of the $^5D_3$ state is longer than that of the $^5D_4$ sate. Hence, the consideration of the $^5D_4$ metastable state is preferable for the analysis of $^5D_3 \rightarrow {}^5D_4$ cross-relaxation. It is possible to put $k_{Td}=k_{Ta}=k_T$ for the case of cross-relaxation between Tb^{3+} ions. The rate equation including the population of $^5D_4$ state is given by

$$\begin{cases} \dfrac{d\rho_d(t)}{dt} = (1-\rho_d(t))\,g - (k_R + k_N)\rho_d(t) - k_T(1-\rho_a(t))\rho_d(t) + \eta_B k_T \rho_a(t)\rho_4(t) \\ \dfrac{d\rho_a(t)}{dt} = k_T(1-\rho_a(t))\rho_d(t) - \eta_B k_T \rho_a(t)\rho_4(t) - k_A \rho_a(t) \\ \dfrac{d\rho_4(t)}{dt} = k_T(1-\rho_a(t))\rho_d(t) - \eta_B k_T \rho_4(t)\rho_a(t) - k_4 \rho_4(t) \end{cases} , \quad \cdots\cdots (39)$$

where $\rho_4(t)$ is the population of $^5D_4$ state and k_4 is the energy relaxation rate of the $^5D_4$ state. The equation for ρ_d in steady-state under a continuous excitation g is

$$k_T(g+k_R+k_N)\{k_4-\eta_B(g+k_R+k_N)\}\rho_d^2+\{(g+k_R+k_N)(k_Ak_4+2\eta_B g k_T)+k_Tk_4(k_A-g)\}\rho_d - g(k_Ak_4-\eta_B g k_T)=0 ,$$

$$\cdots\cdots (40)$$

Solving above quadratic equation of ρ_d, one gets the donor population of Tb^{3+} ions as

$$\rho_d(\infty) = \frac{-(k_R+k_N+g)(k_Ak_4+2\eta_B g k_T)-k_Tk_4(k_A-g)}{2k_T(k_R+k_N+g)\{k_4-\eta_B(k_R+k_N+g)\}} + \frac{\sqrt{\{(k_R+k_N+g)(k_Ak_4+2\eta_B g k_T)+k_Tk_4(k_A-g)\}^2+4k_T(k_R+k_N+g)\{k_4-\eta_B(k_R+k_N+g)\}g(k_Ak_4-\eta_B g k_T)}}{2k_T(k_R+k_N+g)\{k_4-\eta_B(k_R+k_N+g)\}} ,$$

$$\cdots\cdots (41)$$

where k_T is given by equation (31). the fluorescence intensity given by equation (25) is slightly varied due to the presence of η_B. Parameters were evaluated by curve fitting to the experimental results given in Fig.11. The effect of the back-transfer was investigated, comparing the expectations from two analyses with and without the back-transfer. Very little difference were found between them in the steady-state analysis. The reason for it will be that the population of acceptors under excitation from a mercury lamp is enough low for the back-transfer process to be negligible. The population of donors and acceptors were estimated less than 0.01 with these parameters.

The effect of energy back-transfer was expected to appear in the response donor fluorescence under a strong excitation. The decay curves for the Tb^{3+} fluorescence after a pulsed excitation by the N_2-laser excitation were analyzed numerically based on the non-linear model considering the effect of energy back-transfer. It was determined k_R=1000 sec^{-1} and k_4=250 sec^{-1} from the $^5D_3$ and $^5D_4$ decay curves for 0.3mol% of Tb_2O_3. Parameters for the $^5D_3 \rightarrow {}^5D_4$ cross-relaxation were estimated by curve fitting to the experimental results given in

Fig 12. Obtained parameters are listed in table 6. The population of acceptors at t=0 and the non-radiative relaxation rate of donors were assumed to be zero in the analysis, namely $\rho_A(0)=0$ and $k_N=0$. A distance R_0 of 0.4nm was used, which is the minimum distance between two Tb^{3+} ions in Tb_2O_3. The parameters obtained here correspond to those by the steady-state analysis.

The excitation energy of acceptors is dissipated by multi-phonon process [54] In addition to the cross-relaxation between the $^5D_3 \rightarrow {}^5D_4$ and the $^7F_6 \rightarrow {}^7F_0$ transitions, phonon-assisted cross-relaxation to the $^7F_6 \rightarrow {}^7F_1$ and the $^7F_6 \rightarrow {}^7F_2$ transitions were reported [55] Energy diagram and main relaxation processes related to the $^5D_3 \rightarrow {}^5D_4$ cross-relaxation of Tb^{3+} is shown schematically in Fig.22. Taking these transitions to the $^7F_0$, $^7F_1$ and $^7F_2$ levels into consideration, the obtained value of the relaxation rate of acceptors, $k_A \approx 10^4$ at their medium concentration is supported by the report on the multi-phonon relaxation in glasses [56] The estimated dependence of k_A on Tb_2O_3 content can be also understood from the multi-phonon relaxation. With the increase of Tb_2O_3, multi-phonon relaxation will be enhanced. Consequently, k_A will be greatly increased due to the low energy gap between the $^7F_0$ and the $^7F_6$ levels. This interpretation corresponds to the concentration dependence of intensity and lifetime of $^5D_4$ fluorescence [57]. The population density of donors at t=0, $\rho_D(0)$ depends slightly on Tb_2O_3 content in table 6. This reduction of $\rho_D(0)$ is understood as a result of the increased absorption of incident light at high concentration of dopants. The observed red shift of absorption edge of glasses in excitation range [57] is consistent with the concentration dependence of $\rho_D(0)$. The number of Tb^{3+} ions at the second nearest neighbor position is evaluated to be about $4\pi\beta R_0^2 C_d^2 = 3$ at its highest concentration

In order to examine the effect of back-transfer, obtained parameters by present model were compared with those by non-linear model without considering back-transfer and listed in table 7. It can be concluded that the energy relaxation rate of acceptors will be lower estimated by an analysis without taking account of back-transfer. Similar effect of back-transfer was reported for Pr^{3+} ions in a cubic lattice by D.L.Huber et al. [54] based on the Förster theory. The non-linear model with back-transfer gives a fairly good fits, although the fits do not always coincide with the experimental data at higher content of Tb_2O_3. These errors may be mainly caused by

the migration of energy, which were neglected in our analysis. The initial spatial distribution of excitation will change to a spatial equilibrium through migration within the donor system At high concentration of Tb_2O_3, the average donor separation is small and the probability for energy migration between donors is large. The migration leading to a spatial equilibrium may be important at the initial portion of the fluorescence decay of highly doped donors.

The effect of back-transfer on the dynamics of energy transfer from Tb^{3+} to Nd^{3+} ions was also examined using the stochastic model. Curve fittings to the experimental results given in Fig.13 were made by means of a computer simulation. Parameters determined are listed in table 8. The d-q interaction model was still most acceptable for the better fitting to the experimental data. The obtained relaxation rate of acceptors, k_A=1080±100 for the d-q interaction is found about three times greater than that by the stochastic analysis without considering back-transfer. Energy diagram and main relaxation processes related to the energy transfer from Tb^{3+} to Nd^{3+} ions is shown schematically in Fig.23. Acceptors are excited to the state $^4G_{5/2}$ by the energy transfer from Tb^{3+} ions and then relax to the metastable state $^4F_{3/2}$ by emitting phonons. The multi-phonon relaxation to the $^4F_{3/2}$ state and the fluorescence from the $^4F_{3/2}$ state are considered to be dominant for the relaxation of acceptors. Some experimental results [42,43] gave the energy relaxation rate of acceptors as $k_A \approx 2 \times 10^4$ sec^{-1}. The agreement between the theoretical expectation and the experimental data is not perfect. However, the stochastic model considering the energy back-transfer gave an acceptable estimation of the relaxation rate. An agreement in numerical values of obtained parameters means a significant support for the model. Therefore it can be concluded that effect of energy back-transfer should be considered to evaluate the relaxation of acceptors through the measurement of donor fluorescence.

The temperature dependence of the back-transfer was not examined in this study. It will be interesting to investigate the parameter η_B as a function of temperature, since it is suggested that the microscopic rates for backward and forward transfer are in the ratio of $\exp(-\Delta E/kT)$, where ΔE is the energy mismatch .

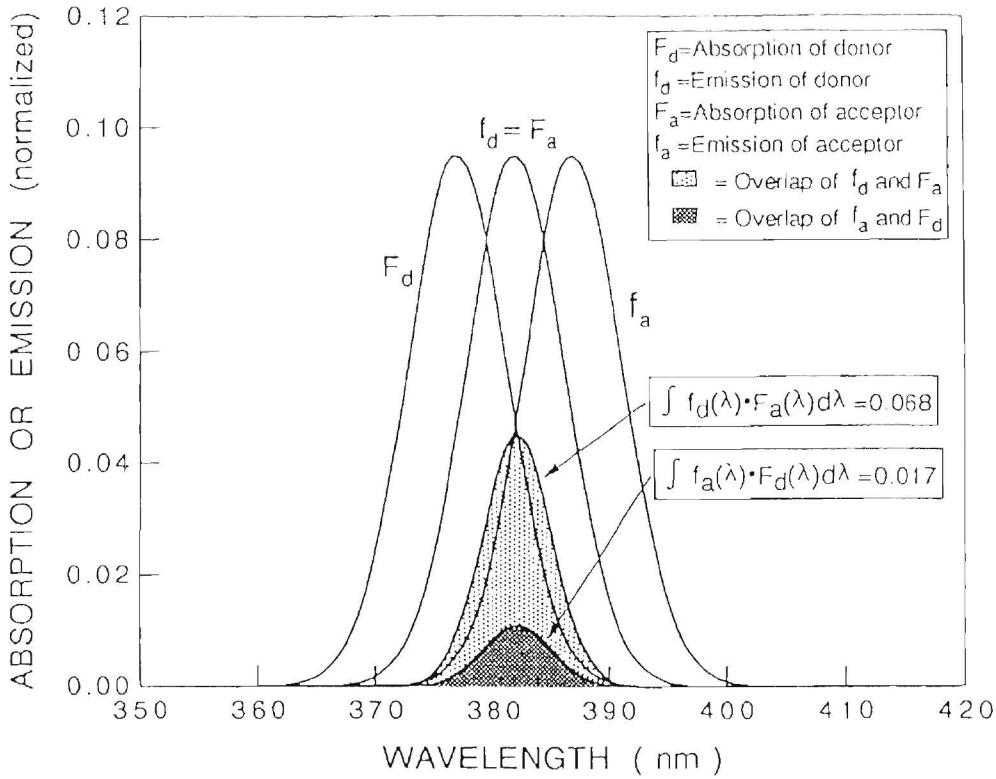

Fig.20. Schematic spectra of absorption and emission for donors and acceptors. The forward and back-transfer rates are proportional to $\int f_d(\lambda) \cdot F_a(\lambda) d\lambda$ and $\int f_a(\lambda) \cdot F_d(\lambda) d\lambda$, respectively. The back-transfer efficiency $\eta_B = 0.2$ is estimated from these overlap integrals, by using a typical data of Tb^{3+} in glasses.

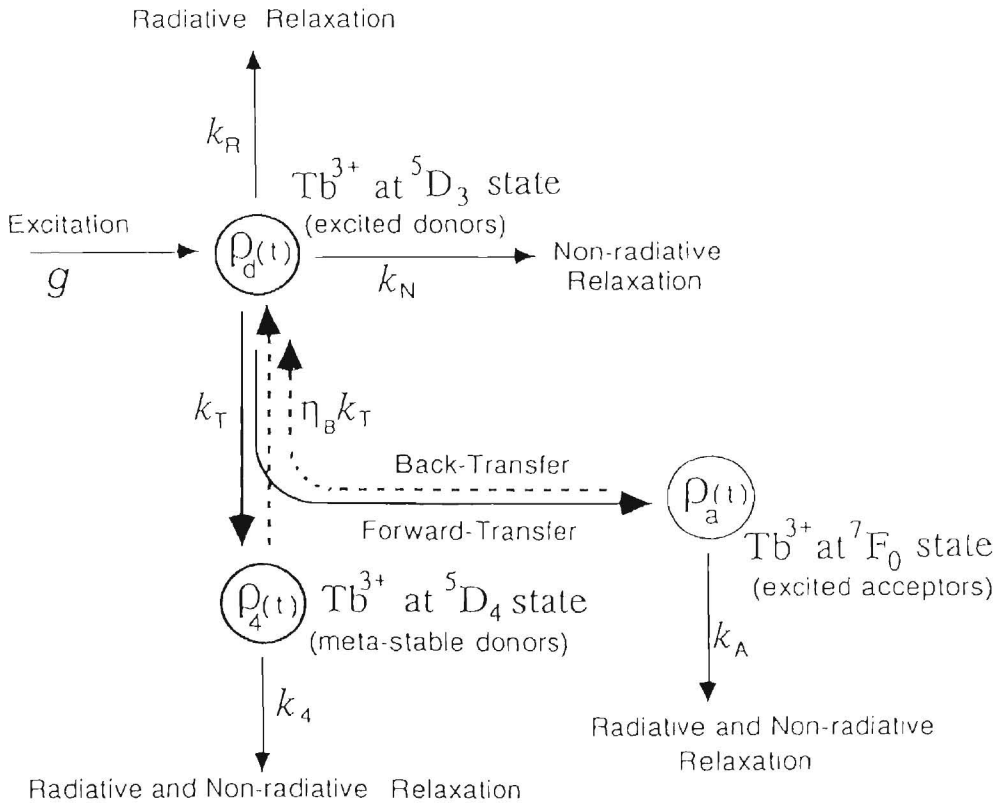

Fig.21. Macroscopic model of energy flow considering the energy back-transfer and the metastable $^5D_4$ state of Tb^{3+} ions

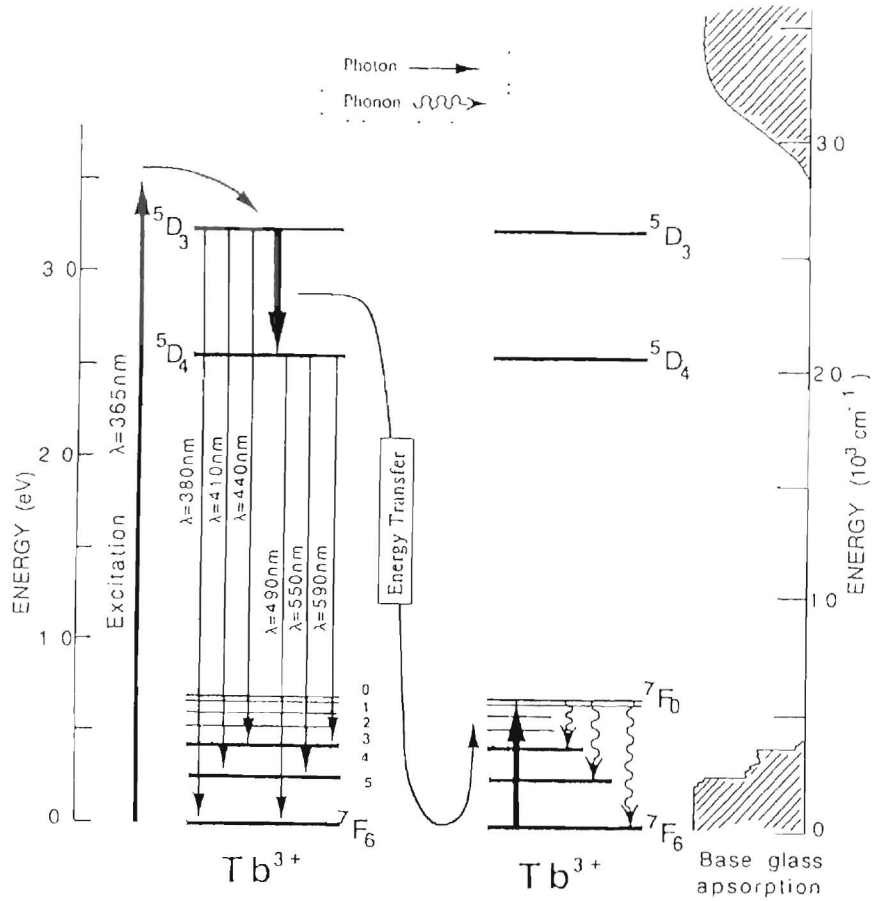

Fig.22. Energy diagram and main relaxation processes of Tb^{3+}.

Table 6. Parameters determined by the non-linear analysis considering the effect of energy back-transfer for the $^5D_3$-$^5D_4$ cross-relaxation of Tb^{3+} ions.

Tb_2O_3 (mol%)	k_R ($10^3 sec^{-1}$)	k_A ($10^3 sec^{-1}$)	R_o (nm)	β ($10^{-36} m^4$)	$p_d(0)$	$p_a(0)$
0.3	1.0	4	1.12	2.0	0.6	0.0
1.0	1.0	5	1.12	2.0	0.6	0.0
1.5	1.0	8	1.12	2.0	0.6	0.0
2.5	1.0	15	1.11	2.0	0.5	0.0
4.0	1.0	25	1.10	2.0	0.4	0.0

Table 7. Comparison of parameters for Tb^{3+} -Tb^{3+} energy transfer determined by analyses with and without considering back-transfer of energy.

Analysis	k_R (sec^{-1})	k_A (sec^{-1})	R_0 (nm)	β (m^4)
with back-transfer	1.0×10^3	$\approx 5\times10^3$	1.12	2×10^{-36}
without back-transfer	1.0×10^3	≤ 100	1.37	2×10^{-36}

k_R : radiative transition rate of donors.
k_A : energy relaxation rate of acceptors.
R_0 : critical distance of energy transfer for a donor-acceptor pair.
β parameter characterizing segregation of donors and acceptors

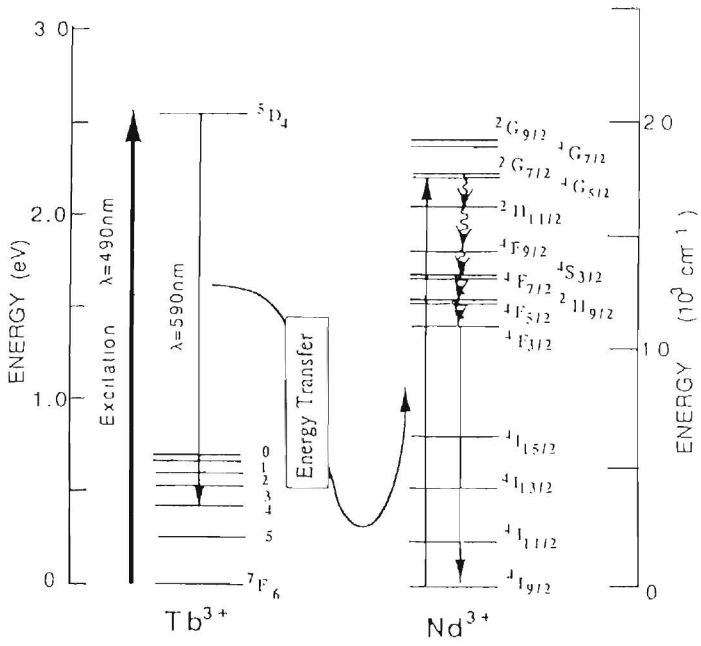

Fig. 23. Energy transfer and main relaxation processes of Nd^{3+}

Table 8. Parameters for the energy transfer between Tb^{3+} and Nd^{3+} ions determined by the stochastic model considering back-transfer of energy.

interaction	d-d	d-q	q-q
dependence on r	-6	-8	-10
k_R (sec^{-1})	430	430	430
k_A (sec^{-1})	< 500	1080±90	> 1700
R_0 (nm)	1.43	1.39	1.41

6. Conclusions

The complex nature of the process of energy transfer between interacting ions in solids makes it difficult to have one general theory which can apply to all physical cases This has led to development of several models to describe specific situations of energy transfer. The major point of this paper is to present a more comprehensive model than the famous Förster model. A model based on a coupled rate equation was developed to remove the difficulties with all Förster-like models. The non-linearity in the rate equation is resulted from the consideration of acceptor excitation, which was disregarded in the Förster model. It was shown that both the non-linear model and the Förster model give good fits to the experimental results in Tb^{3+}-doped glasses. However, theoretical advantages of the non-linear model to all Förster-like models are found Obtaining a good fit between experimental data and the theoretical expectation is not enough to justify the model. Theoretical consistency is another point to evaluate the model. A trial was made to explain the macroscopic behavior of donor fluorescence from the elementary process of energy transfer. Consequently, the non-linear model was developed into a stochastic model in which all probable transitions including energy transfer were stochastically calculated for all donors and acceptors without approximations. The elementary process of energy transfer between a donor-acceptor pair were well connected to the macroscopic response of donor fluorescence in the stochastic model

The Förster model, the non-linear model and the stochastic model were studied to evaluate the origins of the non-exponential decays of donor fluorescence Examining above models, the stochastic model, which is an extension of the non-linear model and the Förster model to include the many-body effect, was found to be the most acceptable model for the donor fluorescence under the influence of energy transfer. Some extra parameters are introduced in the stochastic model, however, they are explicitly treated with physical picture based on the quantum mechanics The non-linearity in the rate equation, discrimination of all active ions and the quantization of transferred energy were essential to the stochastic model Thus it was concluded that the non-exponential responses were caused by the non-linearity in the dynamics of energy transfer. The

macroscopic response of a donor-acceptor system was well constructed from the theory of pair-transfer using two-body expansion. There are many elements to be considered as stated in the previous chapter, however, the quantization of transferred energy will be the most important idea for the detailed modeling of energy transfer. From a theoretical point of view, only the quantization of energy associate with all transitions may be the principle for the energy transfer related phenomena.

Stochastic approaches are required to carry out calculations satisfying the quantization of energy for the modeling. Computer simulations are more useful than analytical method for these stochastic calculations. The Monte Carlo simulation is the best tool for the present, however, it may has some difficulties in practical calculations. Computer simulations considering additional effects such as energy migration and back-transfer of energy might be the case with difficulties. Sine only one transition can be simulated at a time on a computer, the obtained result depends on the algorithm by which all transitions are simulated in a time sequence This logical limitation in the computer simulation seems to be serious to the calculation with additional effects giving less influences on the dynamics of energy transfer. Thus both the computer simulation and the analytical approach will continue to be important also in the future.

Acknowledgments

The author wish to thank Prof. Koji Yamada and Associated Prof. Norihoko Kamata for continuous encouragement and useful suggestions throughout the course of this work.

References

[1] Th Förster, Ann. Physik, 2,55(1948).

[2] Th. Förster, Z. Naturforsch., 4 a,321(1949).

[3] D. L. Dexter, J. Chem. Phys. 2 1,836(1953) .

[4] M. Inokuti and F. Hirayama, J. Chem. Phys. 4 3 ,1978(1965).

[5] M. Yokota and O. Tanimoto, J. Phys. Soc. Jap. 2 2,779(1967).

[6] M.J.Weber, Phy Rev.B 4 , 2932(1971).

[7] W.R.Heller and A.Marcus, Phy.Rev., 8 4,809(1951).

[8] D.K.Sardar and R.C.Powell, J. Lumin 2 2,349(1981).

[9] D.L Huber,Journal of Luminescence 2 8,475(1983).

[10] H.Shiebold and J.Heber, J. Lumin. 2 2,297(1981) .

[11] U.Köbler, Zeitschrift fur Physik,2 5 0 ,217(1972).

[12] L.J.Dowell, Los Alamos National Laboratiry report LA-11873-MS(1990).

[13] H.Dornauf and J.Heber, J. Lumin. 2 2,1(1980).

[14] S.R.Rotman and F.X.Hartmann, Chemical Physics Letters 1 5 2,311(1988).

[15] L. G. Van Uitert and L. F. Johnson,J Chem. Phys., 4 4 ,3514(1966)

[16] E. Nakazawa and S. Shionoya, J. Chem. Phys., 4 7 ,3211(1967).

[17] T.Kim Ahn, T.Ngoc, P.Thu Nga, V.T.Bich P.Long and W.Strek, J. Lumin., 3 9,215(1988).

[18] Marco.Bbettinelli and Ginanluigi Ingletto, J. Lumin. 43,115 (1989)

[19] B.C.Joshi and U.C.Pandey, J.Phys.Chem.Solids.,5 0,599(1989)

[20] K.Tonooka,N.Kamata,K.Yamada,K.Matsumoto,F.Maruyama, J.Lumin.,5 0,139(1991)

[21] D.L.Huber, D.S.Hamilton and B.Barnett, Phys.Rev.B 1 6,4642(1977).

[22] A.Blumen, J Chem. Phys. 7 4,2632(1980).

[31] L. G. Van Uitert, J. Lumin., 4 ,1(1971).

[32] D.J.Robbins, B.Cockayne, B.Lent and J. L. Glasper, Solid State Commun.2 0,673(1976).

[33] L.A.Reisberg and H.W.Moos, Phys.Rev.1 7 4,p429(1968).

[34] T.Miyakawa and D.L.Dexter, Phys.Rev.B 1,p2961(1970).

[35] N.Bodenschatz, R.Wannemacher, J.Weber and D.Mateika, J.Lumin.4 7,159(1991).

[36] C.B.Layne,W.H.Lowdermilk and M.J.Weber, Phys.Rev.B 1 6,10(1977).

[41] K.Tonooka,N.Kamata,K.Yamada,and F.Maruyama, to be published in J.Lumin.

[42] R.R.Jacob and M.J Weber, J.Quantum Electron., QE12 (1976) 102.

[43] C.Barthou and R.B.Barthem, J.Lumin.,46 (1990) 9.

[51] H.Dornauf and J.Heber, J.Lumin. 2 2,1(1980).

[54] D.L.Huber, D.S.Hamilton and B.Barnett, Phys.Rev.B 1 6,4642(1977).

[55] A.Blumen, J.Chem.Phys. 7 4,2632(1980).

[52] B.V.Shulgin, K.N.R.Taylor, A.Hoaksey and R.P.Hunt,J.Phys.C.5 ,1716(1972).

[53] A.Hoaksey , J.Wood and K.N.R.Taylor, J.Lumin.1 7,385(1978).

[54] T.Miyakawa and D.L.Dexter, Phys.Rev.B 1,2961(1970).
[55] N.Bodenschatz, R.Wannemacher , J.Heber and D.Mateika, J.Lumin.47,159(1991).
[56] C.B.Layne,W.H.Lowdermilk and M.J.Weber, Phys.Rev.B 16,10(1977).
[57] K.Tonooka,N.Kamata,K Yamada,K.Matsumoto and F Maruyama,
Proc. int. conf. on science and technology of new glasses, 400 (Tokyo, October 1991).

Appendix

In this appendix, the derivation procedure from equation (17) to equation (18) is explained along with the Förster's treatments. The function J(t) is given by

$$J(t) = \frac{4\pi}{V}\int_0^{R_g} r^2 \exp(- k_R\, t\, R_0^s\, r^{-s})\, dr \qquad \cdots\cdots (17)$$

Here the distribution of acceptors was assumed to be proportional to the square of the distance from a donor to acceptors. Changing the integration variable from r to

$$\zeta = k_R t \left(\frac{R_0}{r}\right)^s \quad , \qquad \cdots\cdots (A1)$$

one can write the function J(t) as

$$J(t) = \frac{4\pi}{V s}(k_R\, t\, R_0^s)^{3/s}\int_{\zeta_g}^{\infty} \zeta^{-1-3/s} \exp(- \zeta)\, d\zeta \qquad \cdots\cdots (A2)$$

where

$$V = \frac{4}{3}\pi R_g^3 \qquad \cdots\cdots (A3)$$

,

and s is 6, 8 and 10 for the dipole-dipole, the dipole-quadrupole and the quadrupole-quadrupole interactions. It is convenient to rewrite in the form

$$J(t) = \frac{3\zeta_g^{3/s}}{s}\int_{\zeta_g}^{\infty} \zeta^{-1-3/s} \exp(- \zeta)\, d\zeta \qquad ,\cdots\cdots (A4)$$

where

$$\zeta_g = k_R t \left(\frac{R_0}{R_g}\right)^s \quad \cdots\cdots (A5)$$

By means of partial integration, one can get the following relation,

$$\int_{\zeta_g}^{\infty} \zeta^{-1-3/s} \exp(-\zeta)\, d\zeta = -\left[\frac{s}{3}\zeta^{-1-3/s}\exp(-\zeta)\right]_{\zeta_g}^{\infty} - \frac{s}{3}\int_{\zeta_g}^{\infty} \zeta^{-3/s}\exp(-\zeta)\, d\zeta$$

$$= \frac{s}{3}\zeta_g^{-1-3/s}\exp(-\zeta_g) - \frac{s}{3}\int_0^{\infty} \zeta^{-3/s}\exp(-\zeta)\, d\zeta + \frac{s}{3}\int_0^{\zeta_g} \zeta^{-3/s}\exp(-\zeta)\, d\zeta \quad \cdots\cdots (A6)$$

We can substitute $\zeta_g \ll 1$ in the integration for a large volume, restricting the analysis to a transient response. Then the definite integral defined by equation (A6) can be approximated to

$$\int_{\zeta_g}^{\infty} \zeta^{-1-3/s}\exp(-\zeta)\, d\zeta = \frac{s}{3}\zeta_g^{-3/s} - \frac{s}{3}\Gamma\left(1-\frac{3}{s}\right) + \frac{s}{3}\frac{s}{s-3}\zeta_g^{1-3/s} + \quad \cdots\cdots (A7)$$

where $\Gamma(x)$ is the Gamma function defined as

$$\Gamma(x) = \int_0^{\infty} \zeta^{-x}\exp(-\zeta)\, d\zeta \quad \cdots\cdots (A8)$$

Neglecting the higher order term than $\zeta_g^{1/2}$ for $\zeta_g \approx 0$ and $s>3$, equation (A6) can be approximated to

$$\int_{\zeta_g}^{\infty} \zeta^{-1-3/s}\exp(-\zeta)\, d\zeta = \frac{s}{3}\zeta_g^{-3/s} - \frac{s}{3}\Gamma\left(1-\frac{3}{s}\right) \quad \cdots\cdots (A9)$$

Utilizing equations (A3) and (A9), we obtain

$$J(t) \approx 1 - \frac{s}{3}\Gamma\left(1-\frac{3}{s}\right)\zeta_g^{1-3/s} \quad \cdots\cdots (A10)$$

Thus the function J(t) containing parameters C_a, R_O, N and k_R was derived as

$$J(t) \approx 1 - \frac{4}{3}\pi C_a R_0^3\, \Gamma(1-3/s)\frac{1}{N}(k_r t)^{3/s} \quad \cdots\cdots (18)$$

And the more, the application of equation (19) to equation (18) would be unsuitable, since the equation (18) is an approximated one neglecting the higher order term than 1/N